

CONTROLS ON GEOCHEMICAL EXPRESSION OF SUBAERIAL EXPOSURE IN ORDOVICIAN LIMESTONES FROM THE NASHVILLE DOME, TENNESSEE, U.S.A.

L. BRUCE RAILSBACK, STEVEN M. HOLLAND, DANIEL M. HUNTER,*
E. MICHAEL JORDAN,† JENNIFER R. DÍAZ,** AND DOUGLAS E. CROWE

Department of Geology, University of Georgia, Athens, Georgia 30602-2501, U.S.A.
e-mail: rlsbk@gly.uga.edu

ABSTRACT: Stable-isotope and trace-element data from 301 samples in six stratigraphic sections largely support previous inferences of subaerial exposure at third-order sequence boundaries in Mohawkian and Cincinnati limestones of the Nashville Dome. They also reveal the presence of previously unrecognized surfaces of subaerial exposure. For example, evidence of subaerial exposure at the tops of parasequences suggests that at least some of the latter are better interpreted as high-frequency sequences. Clusters of surfaces of subaerial exposure near some previously interpreted sequence boundaries suggest that the latter may represent sequence boundary zones. Some surfaces of subaerial exposure are at neither recognized sequence boundaries nor parasequence boundaries and may represent missed beats in which sea-level fluctuations are preserved geochemically but not recognized on stratigraphic criteria. Recognition of these unexpected surfaces of subaerial exposure may in part depend on the close spacing of samples used in this study.

Different sequence boundaries exhibit different degrees of geochemical alteration, and more extensive alteration appears to characterize sequence boundaries of greater temporal significance. Overprinting of exposure surfaces is controlled by accommodation rate, in that meteoric alteration (as suggested by low C isotope composition and Sr concentration) is seemingly pervasive in an interval of slow accommodation but not in an interval of rapid accommodation. $\delta^{18}\text{O}$ values show little relationship to exposure surfaces in these strata, so that Sr- $\delta^{13}\text{C}$ plots are more useful than $\delta^{18}\text{O}$ - $\delta^{13}\text{C}$ plots in recognizing meteoric diagenesis in aggregated data.

In this data set, $\delta^{13}\text{C}$ excursions interpreted to result from pedogenic processes are at most 2.4 ‰ and extend at most only 1.5 meters below exposure surfaces, less than the extent of such signatures in younger carbonates. Such minima are best developed in paleo-lowland and paleo-coastal settings, and they are essentially unrecognizable in paleo-inland settings where more section was removed by lowstand and transgressive erosion.

INTRODUCTION

Sequence stratigraphic principles have increasingly gained acceptance, in part because they foster stratigraphic predictions, such as the location of possible reservoirs and source rocks, condensed sections, and subaerial exposure surfaces. In particular, some subaerial exposure surfaces commonly evaded detection prior to sequence stratigraphy because direct physical evidence of subaerial exposure was obscure (Van Wagoner et al. 1990). For example, Holland and Patzkowsky (1997, 1998) inferred eleven subaerial exposure surfaces in Late Ordovician strata of the Nashville Dome (Tennessee, U.S.A.) on the basis of sequence architecture. Each of these surfaces occurs at a third-order sequence boundary delimiting a type I sequence

(*sensu* Van Wagoner et al. 1990) and was recognized principally by the abrupt shift from progradational stacking in the inferred highstand systems tract to retrogradational stacking in the transgressive systems tract. Although some of these surfaces display regional truncation of underlying strata, most are nondescript in individual outcrops, with features such as paleokarst and paleosols rarely evident. The scarcity of subaerial exposure features raises the question of whether the sequence architecture was correctly inferred, or whether these sequences are type II sequences lacking subaerial exposure and containing shelf-margin systems tracts impossible to distinguish from the underlying highstand systems tract (Fig. 1; see Posamentier and James 1993).

This question has motivated us to look for diagenetic or geochemical evidence of subaerial exposure at these inferred sequence boundaries. When compared to strata of other ages, Ordovician carbonates have many characteristics that do not favor recognition of meteoric diagenesis. The lack of a flora of vascular plants dictated that soil development was not as extensive as in later periods, and that sequestration of ^{13}C -depleted CO_2 into diagenetic carbonates was minimized. Furthermore, if the P_{CO_2} of the Ordovician atmosphere was 12 to 20 times as great as that of today (Bernier 1994), atmospheric CO_2 in soils would have diluted biologically fractionated CO_2 much more than after the large Devonian decrease in atmospheric

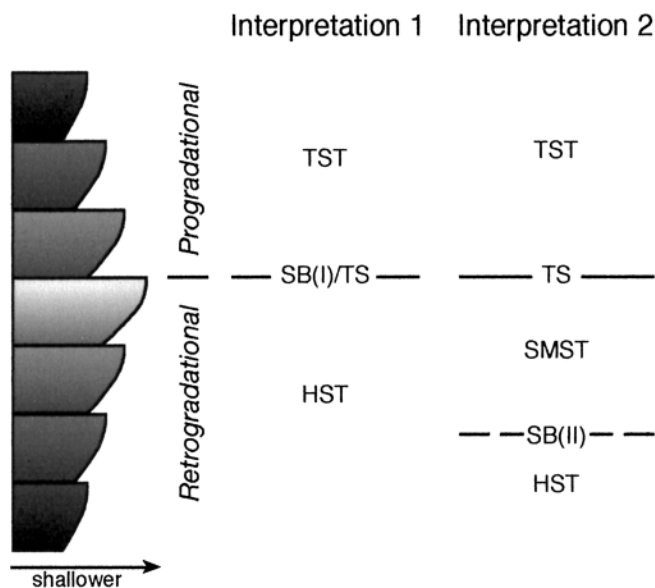


Fig. 1.—Alternative explanations of strata exhibiting progradational followed by retrogradational stacking. In Interpretation I, the switch in stacking patterns is interpreted as a combined type I sequence boundary (SB(I)) and transgressive surface (TS), underlain by the highstand systems tract (HST) and overlain by the transgressive systems tract (TST). In Interpretation II, the switch in stacking patterns marks only the transgressive surface and is overlain by the transgressive systems tract. A type II sequence boundary (SB(II)) lies somewhere below the transgressive surface and separates the shelf-margin systems tract (SMST) from the underlying highstand systems tract; the SB in this case is not manifested by any obvious change in lithofacies or stacking patterns. See Posamentier and James (1993) for an extended discussion of the relationships between type I and type II sequences.

* Present address: Clayton Group Services, 3380 Chastain Meadows Parkway, Suite 300, Kennesaw, Georgia 30144, U.S.A.

† Present address: College of Education, University of Georgia, Athens, Georgia 30602 U.S.A.;

** Present address: Jacobs Engineering Group, 318 East Inner Road, Otis ANG Base, Buzzards Bay, Massachusetts 02542, U.S.A.

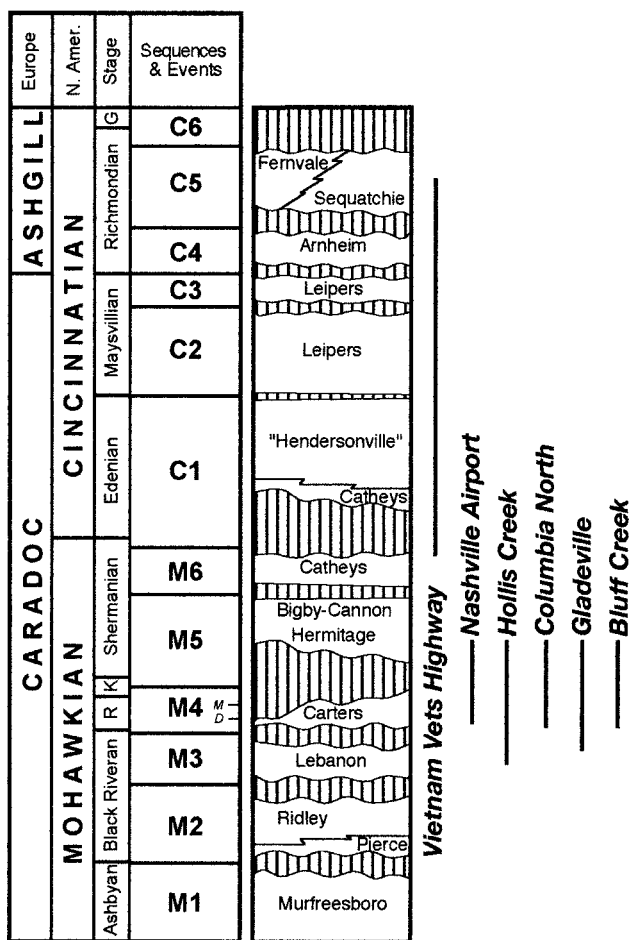


FIG. 2.—Sequence stratigraphy and lithostratigraphy of the Upper Ordovician of the Nashville Dome (based on Holland and Patzkowsky 1998). Sequences M1 through M6 lie within the Mohawkian Series and C1 through C6 lie within the Cincinnati Series. The C6 sequence occurs farther north along the Cincinnati Arch, but is not present on the Nashville Dome. “D” and “M” in the Sequences and Events column represent the Deicke (T3) and Millbrig (T4) K-bentonites. “R,” “K,” and “G” in Stage column represent Rocklandian, Kirkfieldian, and Gama-chian. Vertical dashed lines in the lithostratigraphy column represent inferred times of subaerial exposure and erosion. The stratigraphic extent of the sections used in this study is indicated on the right.

CO₂. In addition to issues concerning CO₂, scarcity of primary aragonite during a calcitic phase in the mineralogy of abiotic carbonates (Sandberg 1983; Wilkinson and Given 1986) and micrite (Lasemi and Sandberg 1994) means that the diagenetic potential of Ordovician carbonates would have been less than that of limestones deposited during times of aragonitic oceans. These factors, combined with the considerable age of Ordovician limestones and thus their significant susceptibility to later diagenesis, suggest that it might be difficult to recognize evidence of early meteoric diagenesis to test the presence of surfaces of subaerial exposure. Although meteoric cements have been recognized previously in Ordovician limestones of eastern North America (e.g., Grover and Read 1983; Tobin and Walker 1994; Kher 1996; Brown 1997), this paper is concerned with geochemical identification of exposure surfaces within stratigraphic sections and over regional scales.

In addition to these concerns about recognizing early meteoric diagenesis in carbonates from the Ordovician, Whitaker et al. (1997) have argued that carbonates of all ages are subject to diagenetic overprinting during repeated cycles of rise and fall of sea level. Their model, which invoked Quaternary fluctuations of sea level and typical Quaternary aragonite-rich shallow ma-

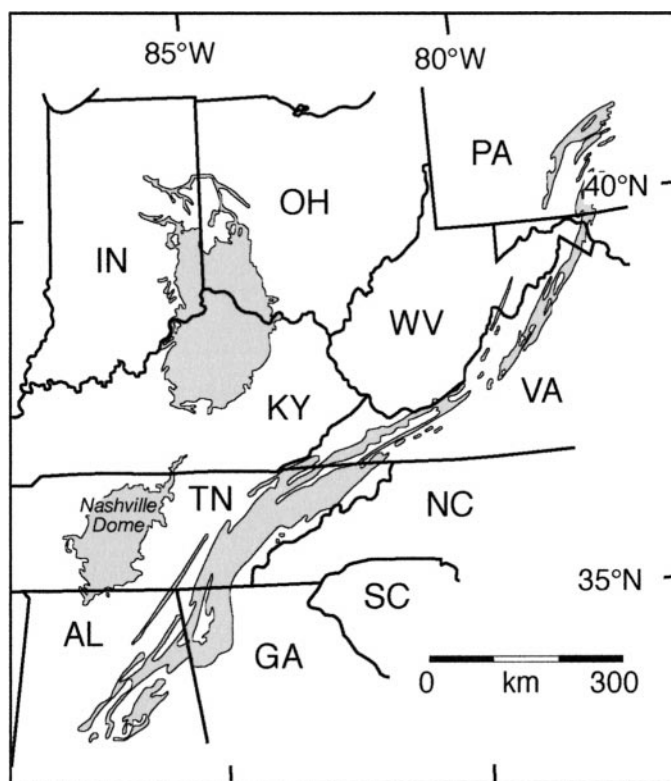


FIG. 3.—Map of the Ordovician outcrop area (shaded) in the eastern United States, with the location of the Nashville Dome indicated.

rine sediments as its inputs, showed that zones of maximal meteoric diagenesis might be displaced from unconformities as any one horizon was subjected to multiple episodes of meteoric diagenesis of varying duration. This effect might be especially profound in intervals with small accommodation rates, because any one horizon would remain near the exposed land surface longer. Thus one might question whether meteoric diagenesis would be of use in evaluating proposed sequence boundaries of cratonic carbonates of any age, and especially those of Ordovician age.

In light of these issues, this paper examines geochemical and petrographic evidence for meteoric diagenesis at interpreted sequence boundaries in the Ordovician of the Nashville Dome. In doing so, it seeks to address four questions: (1) Can we recognize meteoric diagenesis and subaerial exposure at Holland and Patzkowsky’s (1997, 1998) stratigraphically defined boundaries?; (2) Can we recognize other surfaces of subaerial exposure in these strata, and thus go beyond the limits of a purely sequence stratigraphic approach?; (3) Does our ability to recognize surfaces of subaerial exposure and sequence boundaries differ between intervals of rapid and slow accommodation because of varying degrees of overprinting?; and (4) How does expression of subaerial exposure vary laterally?

To address the questions above, we studied six outcrops that expose collectively seven previously recognized sequence boundaries; in all, twelve exposures of sequence boundaries were examined. For our systematic analysis of geochemical signals, we used micrites wherever possible, because the large surface area and possibly metastable original mineralogy of micrite makes it a good candidate for alteration during early diagenesis. We sampled at decimeter-to-meter scale, rather than at the meter-to-multiple-meter scale commonly used (e.g., Beeunas and Knauth 1985; Algeo 1996; Fouke et al. 1996). Our results indicate that surfaces of subaerial exposure can be recognized, commonly in greater abundance than that predicted by sequence stratigraphic analyses alone, but that recognition of

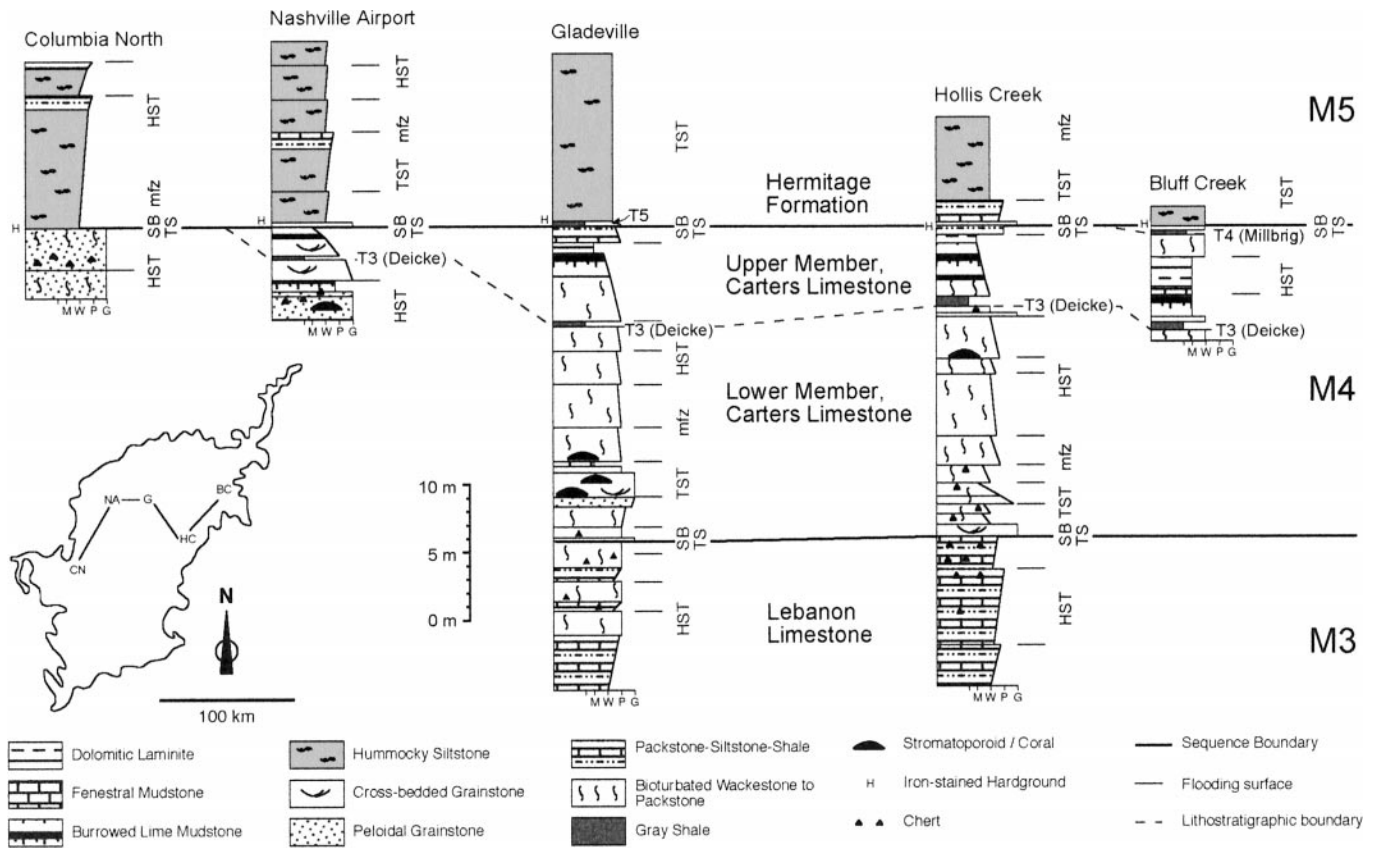


FIG. 4.—Sequence stratigraphic correlation of M3–M5 exposures used in this study, adapted from Holland and Patzkowsky (1998). Inset map of the Nashville Dome outcrop belt indicates locations of these outcrops. Complete locality information, as well as facies descriptions and stratigraphic interpretations, are given in Holland and Patzkowsky (1997, 1998). HST: Highstand systems tract. TST: Transgressive systems tract. SB: Sequence boundary. TS: Transgressive surface. mFz: Maximum flooding zone. T3, T4, and T5 are widely correlated K-bentonites.

exposure varies greatly with several geographic and stratigraphic parameters.

STRATIGRAPHIC SETTING

Eleven third-order depositional sequences, each spanning 1–3 million years, have been described from Upper Ordovician strata of the Nashville Dome (Fig. 2, 3; Holland and Patzkowsky 1997, 1998). From lowest to highest, these are numbered M1 to M6 for those in the Mohawkian Series and C1 to C5 for those in the Cincinnati Series; all sequence boundaries are named here for the overlying sequence. Each consists of a retrogradational set of parasequences, forming the transgressive systems tract (TST), and an overlying progradational set of parasequences, forming the highstand systems tract (HST). Some of the sequence boundaries display evidence of regional truncation (M5, C5, Ordovician–Silurian boundary), chertification (M2, M3, M4, M5), and diagenetic mottling (M5, C1, C2). Minor paleokarst features have been recognized at some outcrops of the M4, M5, M6, and C5 sequence boundaries, as well as the Ordovician–Silurian boundary, in the form of teepee-like deformation, scalloped and overhanging surfaces, and 1-cm-wide fissures. Each of these sequence boundaries is merged with a transgressive surface and thus commonly displays features associated with transgression, such as borings, hardgrounds, pyritization, phosphatization, and skeletal and intraclastic lags.

Upper Ordovician rocks of the Nashville Dome consist mainly of carbonates, with varying proportions of thin intervals, beds, and partings of siliciclastic mudstone. The M1 through M4 sequences are characterized by tropical-type carbonates that contain abundant micrite, a wide diversity of

allochests (including abundant peloids and uncommon ooids), common hardgrounds, and a warm-water fauna (Holland and Patzkowsky 1997; Patzkowsky and Holland 1999). The C1 through C5 sequences are characterized by temperate-type carbonates that lack abundant micrite, contain almost exclusively bioclastic allochests, and display a cool-water fauna. In contrast to the M1 to M4 sequences, the C1 to C5 sequences contain abundant siliciclastic mud and phosphate. The M5 and M6 sequences represent conditions transitional between these two extremes. This switch following the M4 sequence, which affects all bathymetric sedimentary environments on the Nashville Dome, has been interpreted as reflecting the onset of upwelling driven by favorable wind fields and the formation of the Appalachian Basin to the east of the Nashville Dome during the Taconic Orogeny near the beginning of the M5 sequence (Holland and Patzkowsky 1997, 1998). The Nashville Dome was situated at approximately 20° S throughout the Late Ordovician.

Backstripping analysis of these sequences revealed a four-fold drop in accommodation rates, beginning with the C1 sequence (Holland and Patzkowsky 1998), with long-term rates of 18.0 m/My during the M2 through M6 and 4.4 m/My during the C1 through C6. Because coeval strata to the north along the Cincinnati Arch do not display a similar drop in accommodation rates, this switch was interpreted to reflect a decrease in subsidence rates on the Nashville Dome.

Six sections or local composite sections were examined in this study (Figs. 4–5). All are recent road cuts. Bluff Creek, Columbia North, and Nashville Airport all expose the M5 sequence boundary (Fig. 4). Gladeville and Hollis Creek expose the M4 as well as the M5 sequence boundary.

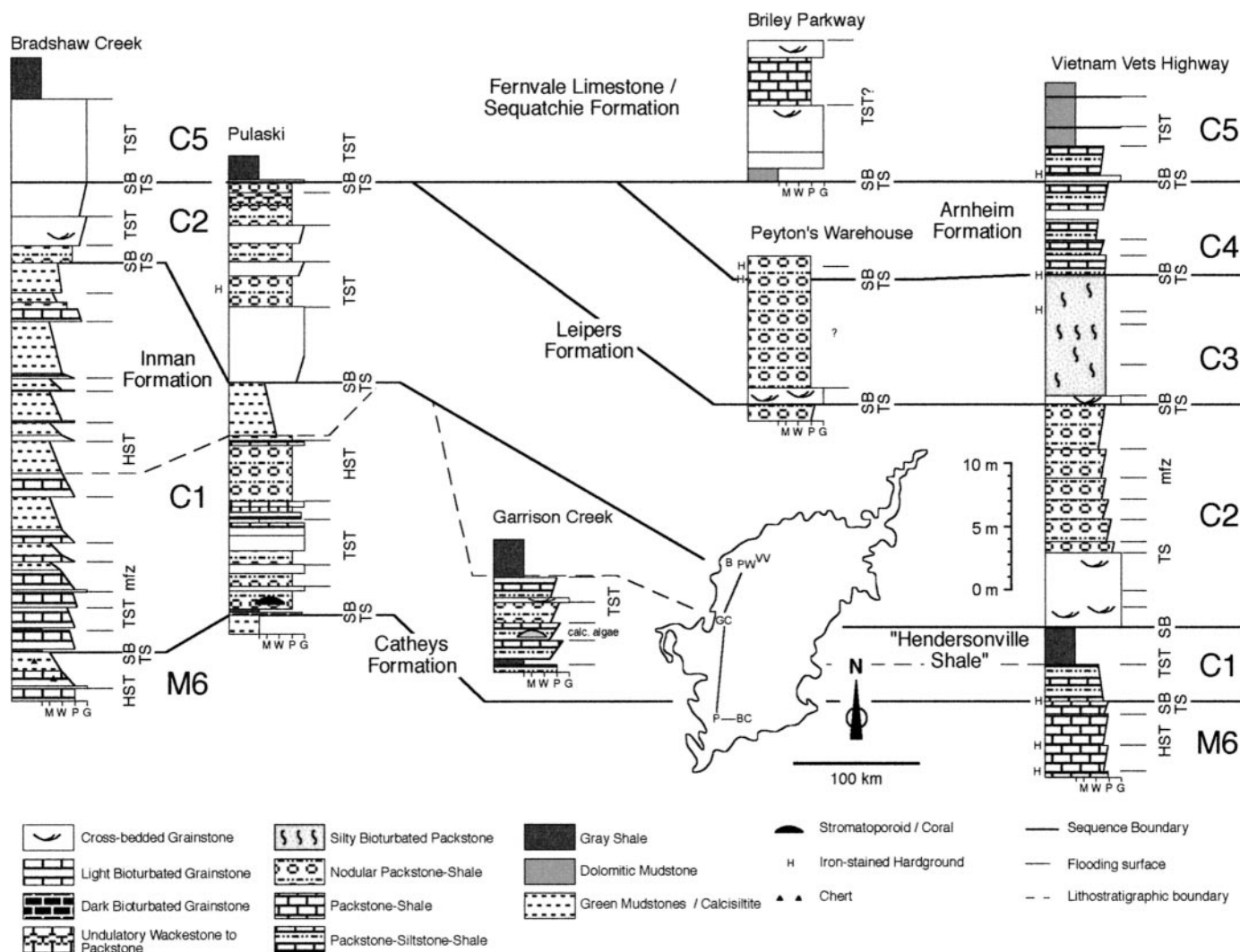


FIG. 5.—Sequence stratigraphic context of the M6–C5 sequences; only the Vietnam Vets Highway outcrop was used in this study. Figure adapted from Holland and Patzkowsky (1998). See caption of Figure 4 for explanation.

Comparison with the Ordovician–Silurian flank of the Nashville Dome shown in figure 10 of Stearns and Reesman (1986) suggests that Columbia North was the most inland of these M4–M5 locations in the Ordovician. The Vietnam Vets Highway road cut, on the other hand, exposes the C1 through C5 sequence boundaries (Fig. 5) and was in a relatively basinward location (again relative to the Ordovician–Silurian flank of the Nashville Dome shown in figure 10 of Stearns and Reesman 1986).

METHODS

Sample Preparation and Chemical Analysis

Hand samples were collected from road cuts at roughly 10 cm intervals in the 2 to 3 m below interpreted sequence boundaries and in the 1 m above, and they were generally collected at 1 m intervals farther from such boundaries. Powdered subsamples of micrite or micrite-rich material (as identified on cut surfaces or in matching thin sections) were, wherever possible, obtained from these samples using a dental drill, with slow drilling speeds used to minimize possible recrystallization and isotopic fractionation. Where no micrite was present, an undifferentiated sample was pulverized to generate a powder for analysis. Comparisons within the data

show no systematic geochemical difference between micrite and bulk samples, as was also found by Díaz (1996).

CO₂ was extracted from samples for isotopic analysis using the phosphoric acid method of McCrea (1950) and was analyzed using either a Finnegan Delta E or Finnegan MAT 252 mass spectrometer in the University of Georgia Department of Geology Stable Isotope Laboratory. Samples were reacted at 50°C, and the reported δ¹³C and δ¹⁸O values were corrected to 25°C using the equation of Swart et al. (1991). Harding Iceland Spar was used as a laboratory standard. Precision is better than ± 0.1‰ for both δ¹³C and δ¹⁸O. Isotopic data are therefore reported to one decimal place, whereas means of data are reported to two decimal places. Isotopic data are reported in Appendix 1, which can be accessed in the JSR digital data repository (see Acknowledgments).

Subsamples of the same powders were reacted with HCl and analyzed in solution using a Thermo Jarrell-Ash 965 inductively coupled argon plasma (ICP) spectrometer in the University of Georgia Chemical Analysis Laboratory. Elemental concentrations of Sr in calcite are reported here using Sr/Ca ratios and assuming 40.0 wt% Ca in Mg-free calcite or proportionately lower Ca concentrations in Mg-bearing calcites. The Thermo Jarrell-Ash 965 ICP results have standard errors of 0.46% for Ca, 0.30% for

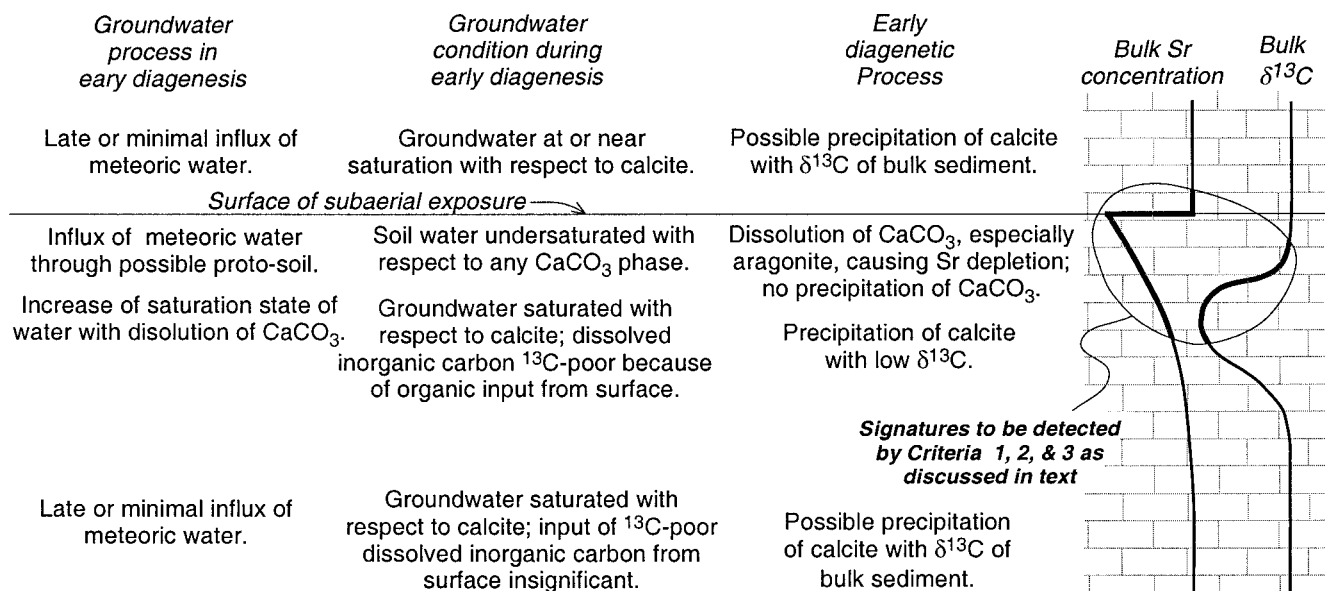


Fig. 6.—Conceptual model illustrating why Criteria 1 and 2 discussed in text involve a zone of lesser Sr concentration that potentially lies above the minimum in $\delta^{13}\text{C}$ beneath a surface of subaerial exposure.

Mg, and 0.48% for Sr, which yields a standard error of 1%, or 0.0004 wt% Sr. Our replicate analyses yield differences in Sr concentration of 0.001 wt % Sr.

Mol % MgCO_3 was calculated as the concentration of Mg divided by the sum of the concentrations of Ca, Mg, and Fe. Samples with Mg concentrations greater than 5 mol % MgCO_3 were excluded from the data set because they presumably contain significant dolomite. This procedure eliminated 88 of 389 original samples. Elemental data from ICP analysis are reported in Appendix 1.

Thin sections of most hand samples were prepared and examined using a Leitz Laborlux 12 Pol S petrographic microscope equipped with a Nuclide ELM 3UR cathodoluminescence. Detailed chemical analyses, largely of cements with zoning revealed by cathodoluminescence, were performed on polished C-coated thin sections using the University of Georgia Department of Geology's JEOL JXA 8600 electron microprobe with wavelength-dispersive spectrometers. Results of these analyses, as well as details of the procedures, are reported in Díaz (1996), Jordan (1999), and Hunter (2000).

Criteria for Recognition of Surfaces of Subaerial Exposure

We used three levels of criteria to recognize possible surfaces of subaerial exposure. These were based on three assumptions: (1) that subaerial exposure results in dissolution of aragonite and thus depletion of Sr below the exposure surface; (2) that subaerial exposure results in precipitation of CaCO_3 with pedogenically induced low $\delta^{13}\text{C}$ values below the exposure surface; and (3) that the zone of supersaturation with respect to CaCO_3 and resultant precipitation of ^{13}C -poor calcite may lie slightly below the zone of undersaturation and aragonite dissolution (Fig. 6). Criterion 1 therefore was chosen as a decrease in Sr concentration of 0.01 wt. % from any given sample to the one below and a decrease in $\delta^{13}\text{C}$ of 1.0‰ downward between those two samples or from the lower of those two samples to the sample below it. Criterion 2, less stringent than Criterion 1, requires a decrease in Sr concentration of 0.005 wt. % from any given sample to the one below and a decrease in $\delta^{13}\text{C}$ of 0.5‰ downward between those two samples or from the lower sample to the sample below it. Criterion 3, the least stringent, requires only a decrease in $\delta^{13}\text{C}$ of 0.5‰ from one sample to that below it. Criterion 3 thus follows previous work (e.g., Goldstein

1991; Algeo 1996) in using only C isotopes as an indicator of subaerial exposure, whereas Criteria 1 and 2 additionally require a change in Sr concentration.

RESULTS

M3 to M5 Sequences

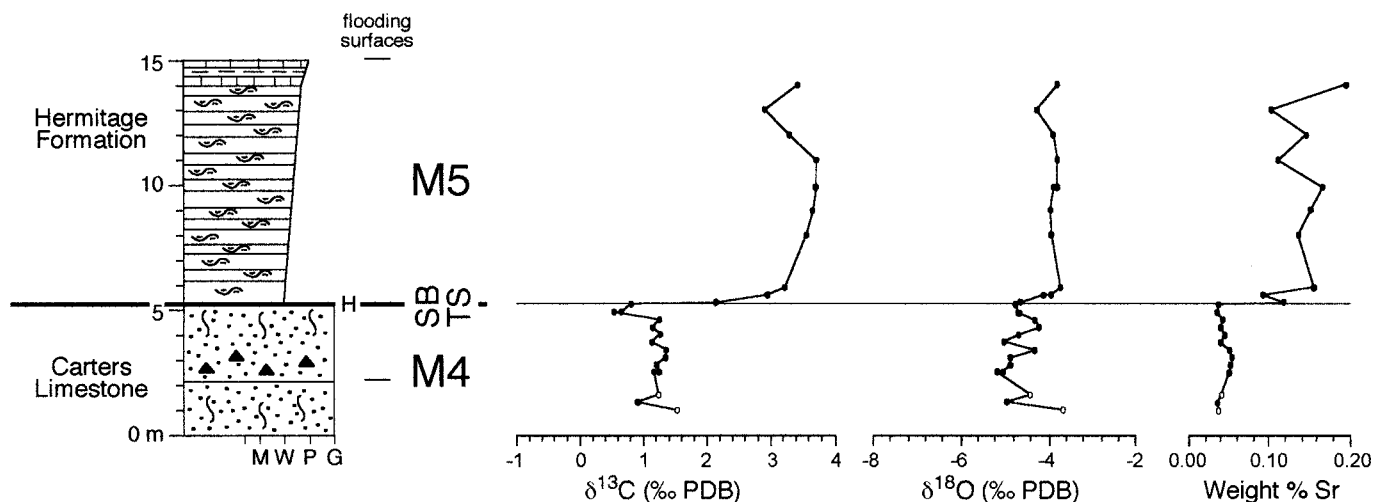
$\delta^{13}\text{C}$ values of all samples below the M5 sequence boundary range from -1.1 to $+1.7$ ‰ relative to PDB (Figs. 7–11). These values generally increase upward slightly, but they are lowest just below the M5 sequence boundary at Hollis Creek and Gladeville. In contrast, $\delta^{13}\text{C}$ values above the M5 sequence boundary range from 0.9 to 3.7‰, with the greatest values at Columbia North and Nashville Airport (Figs. 7–11). The only exception to this range is a sample from an obvious intraclast of Carters Limestone (M4) at Gladeville, which has a $\delta^{13}\text{C}$ value of -0.7 ‰, similar to that of uppermost samples in the M4 sequence.

$\delta^{18}\text{O}$ values of all samples in the M3 through M5 sequences range from -6.0 to -2.2 ‰ relative to PDB (Figs. 7–11). The greatest single value is from just below the T3 (Deicke) K-bentonite and may be the result of a hydrologically sequestered location in which water-rock interaction was minimized. At Columbia North and Nashville Airport, $\delta^{18}\text{O}$ values are generally greater above the M5 sequence boundary than below it. $\delta^{18}\text{O}$ values otherwise show little regular stratigraphic variation. Values of $\delta^{18}\text{O}$ correlate with $\delta^{13}\text{C}$ at Hollis Creek in the four meters above the T3 K-bentonite (Fig. 9), but elsewhere the two rarely correlate.

Sr concentrations determined by ICP analysis of dissolved powders range from 0.017 to 0.196 wt. % (Figs. 7–11). Like the $\delta^{13}\text{C}$ values, Sr concentrations are generally greater above the M5 sequence boundary than below it, except in the M4-derived intraclast in the basal M5 at Gladeville and in samples just above the boundary at Nashville Airport and Bluff Creek.

Recognition of Subaerial Exposure in Sequences M3 to M5

Five instances in the M3–M5 data meet Criterion 1 for recognition of surfaces of subaerial exposure (see Methods). All five occur at the M5 sequence boundary (Figs. 7–11). Four more instances fail to meet Criterion 1 but meet Criterion 2. Two of those are at correlative parasequence tops



Columbia North

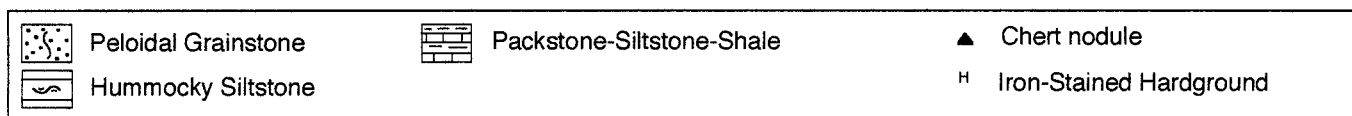
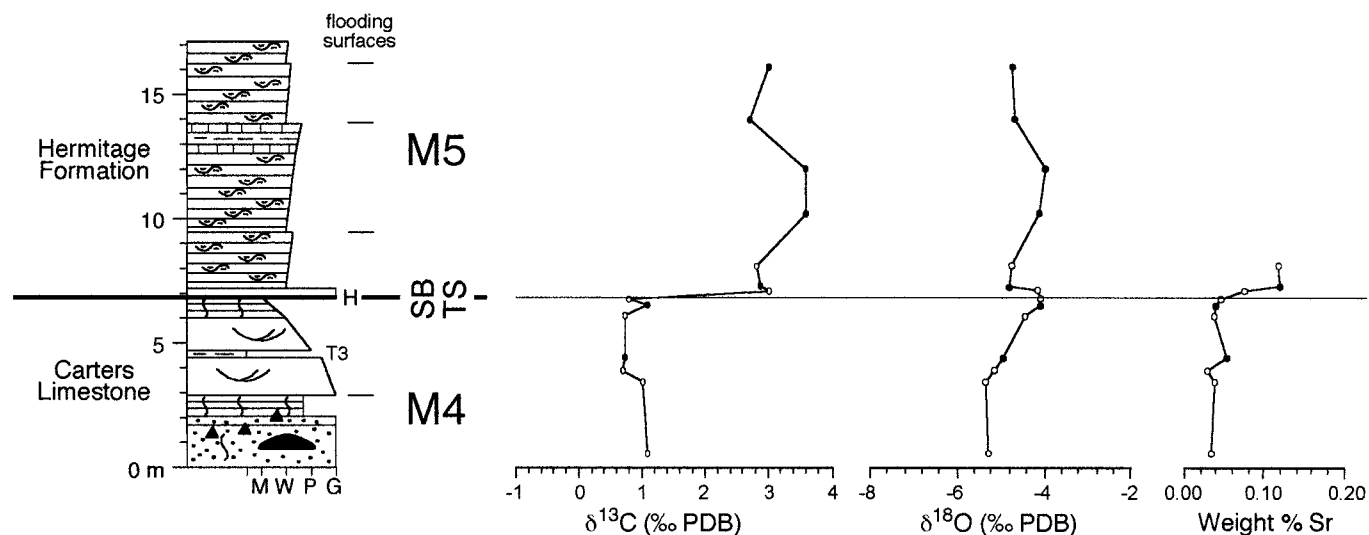


FIG. 7.—Stable C and O isotope composition and Sr concentration of limestone in the M4 and M5 sequences at the Columbia North locality near Columbia, Tennessee. Analytical uncertainty of isotopic and elemental results is less than width of symbols shown. Most data are from micrite (filled symbols); data from micrite-free rocks are shown with open symbols. Sequence boundaries and flooding surfaces shown at left are based on the work of Holland and Patzkowsky (1997, 1998) prior to this study; the location of their surfaces was not based on the geochemical criteria used in this study. Solid horizontal lines indicate surfaces of subaerial exposure inferred using Criterion 1, dashed lines indicate surfaces satisfying Criterion 2, and dotted lines indicate surfaces satisfying Criterion 3. Spacing of samples shown is locally greater than that of samples collected because of removal of Mg-rich samples from data (see Methods).



Nashville Airport

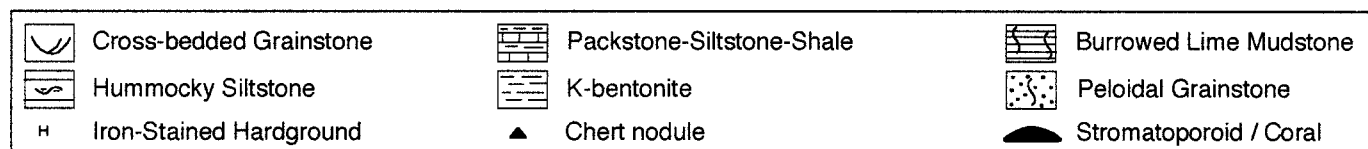
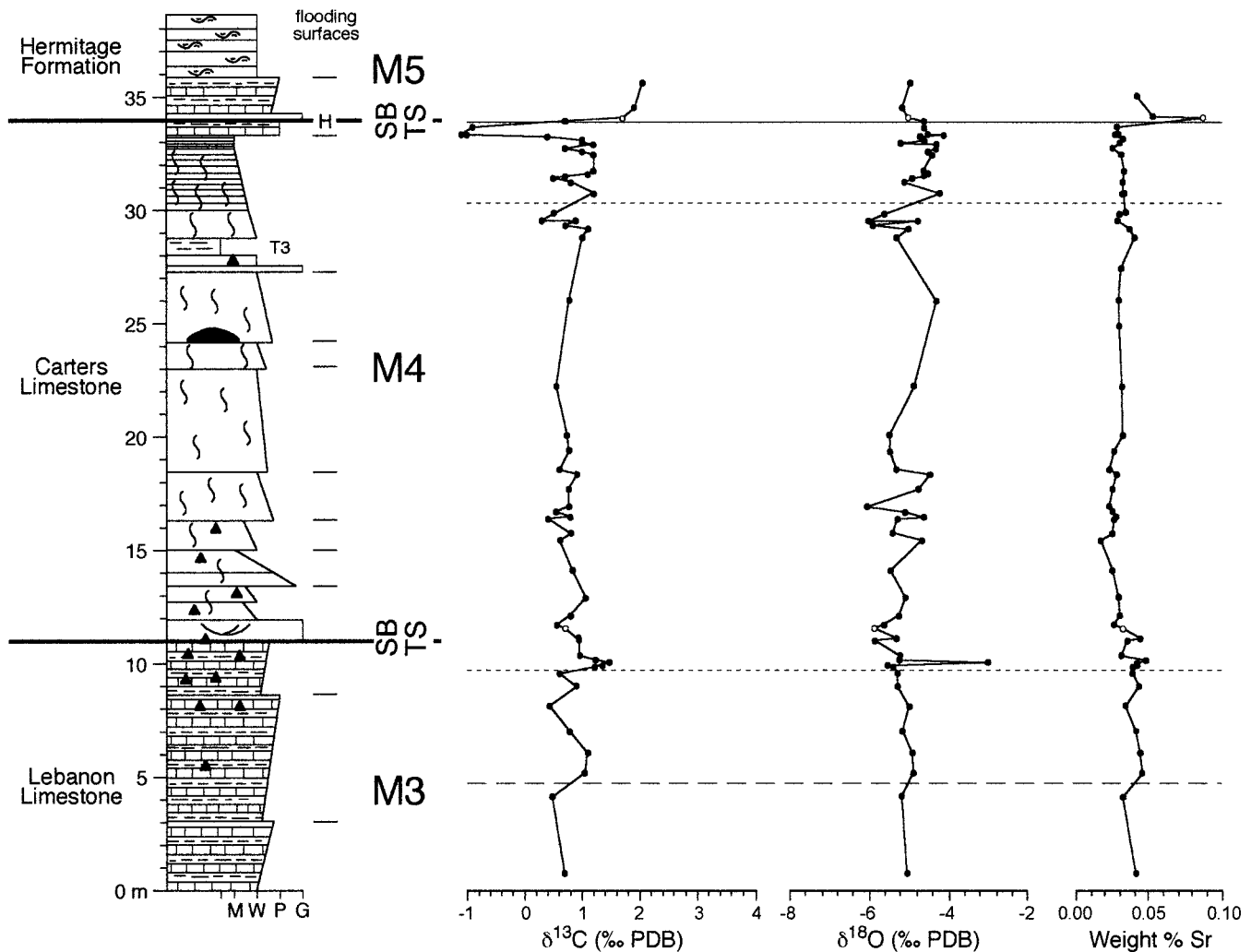


FIG. 8.—Stable C and O isotope composition and Sr concentration of micritic limestone in the M4 and M5 sequences at the Nashville Airport locality near Nashville, Tennessee. See caption of Figure 7 for explanation.



Hollis Creek

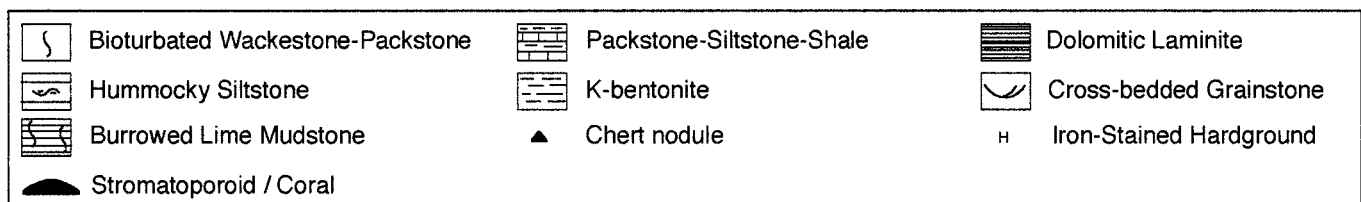


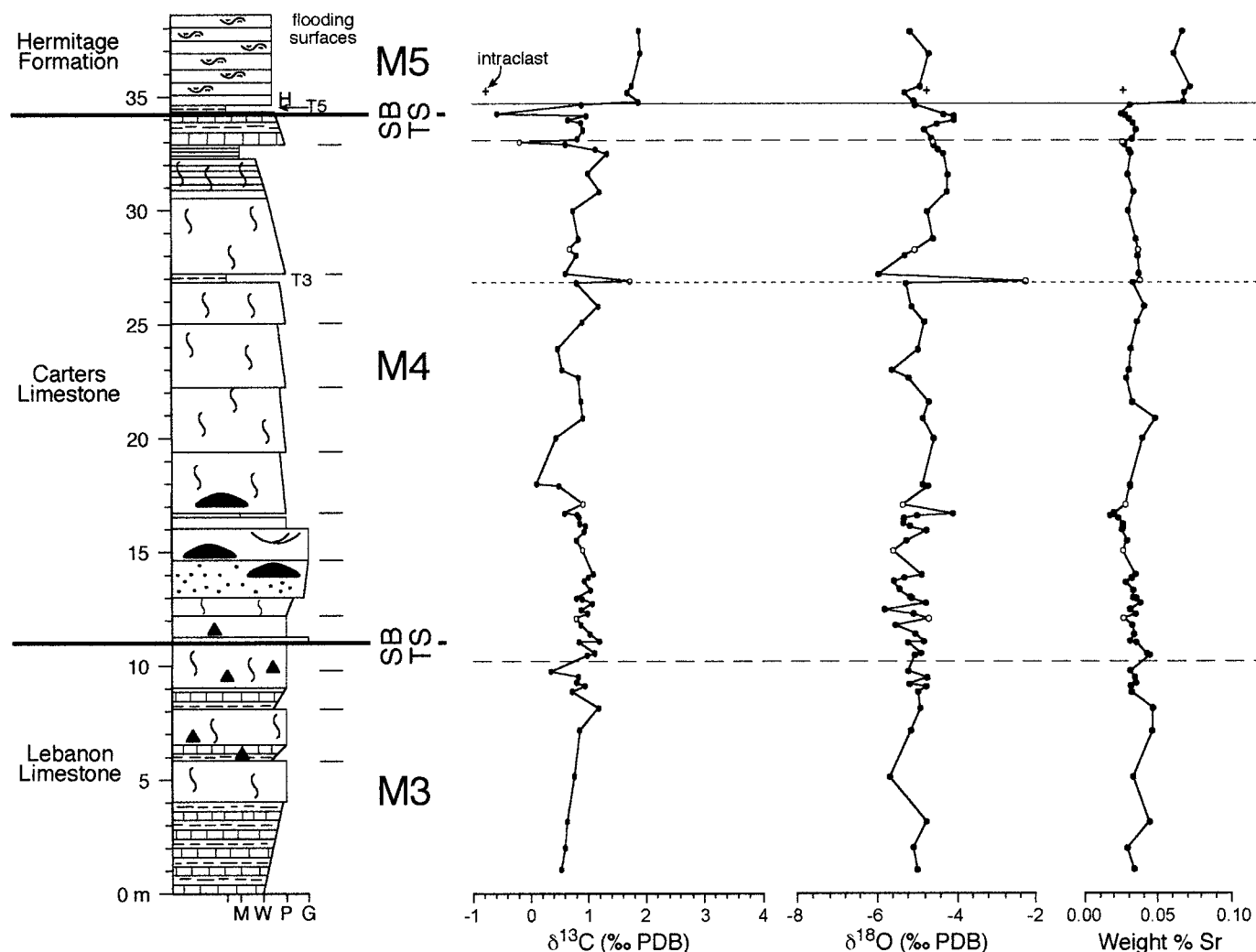
FIG. 9.—Stable C and O isotope composition and Sr concentration of micritic limestone in the M3 to M5 sequences at the Hollis Creek locality near Woodbury, Tennessee. See caption of Figure 7 for explanation.

in the M4 sequence at Gladeville and Bluff Creek. A third is below, but not at, the M4 sequence boundary at Gladeville, and the fourth is in the M3 sequence at Hollis Creek. Three further instances fail to meet Criteria 1 and 2 but meet Criterion 3. One is below the T3 (Deicke) K-bentonite at Gladeville and may be a spurious result from an anomalously high $\delta^{13}\text{C}$ value just below the bentonite. A second is high in the M4 sequence at Hollis Creek but below the parasequence boundary discussed above. The third is just below the M4 sequence boundary at Hollis Creek, and thus is correlative with the horizon meeting Criterion 2 below the M4 sequence boundary at Gladeville.

M6 to C5 Sequences

$\delta^{13}\text{C}$ values of all samples in the M6 through C5 sequences range from -2.6 to $+0.5$ ‰ relative to PDB (Fig. 12). However, the mean value below the C4 sequence boundary is -0.67 ‰, whereas the mean value above that boundary is -0.14 ‰. The means differ significantly (Student's $t = 5.871$, $n_1 = 75$, $n_2 = 25$, $p \ll 0.001$). $\delta^{13}\text{C}$ values of samples in the M6 through C5 sequences are lower than those of almost all samples in the M3 through M5 sequences (Fig. 13).

$\delta^{18}\text{O}$ values of all samples in the M6 through C5 sequences range from



Gladeville

	Bioturbated Wackestone-Packstone		Packstone-Siltstone-Shale		Dolomitic Laminite
	Hummocky Siltstone		K-bentonite		Cross-bedded Grainstone
	Burrowed Lime Mudstone		Peloidal Grainstone	H	Iron-Stained Hardground
	Stromatoporeid / Coral		Chert nodule		

FIG. 10.—Stable C and O isotope composition and Sr concentration of micritic limestone in the M3 to M5 sequences at the Gladeville locality near Lebanon, Tennessee. See caption of Figure 7 for explanation.

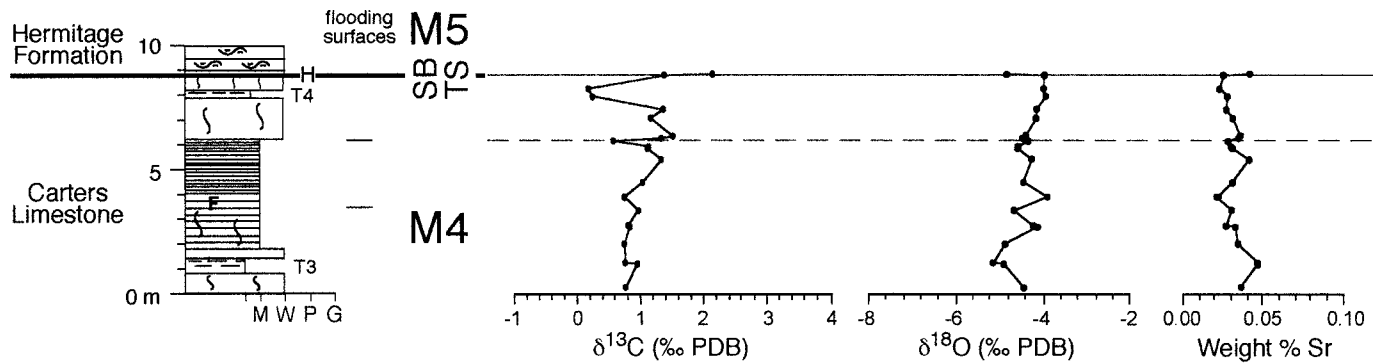
−7.2 to −2.2 ‰ relative to PDB (Fig. 12). The mean value below the C4 sequence boundary is −4.80, whereas the mean value above that boundary is −4.51 ‰. The means do not differ significantly (Student's $t = 1.846$, $n_1 = 75$, $n_2 = 25$, $p = 0.068$). The two lowest $\delta^{18}\text{O}$ values coincide with low $\delta^{13}\text{C}$ values. The range of $\delta^{18}\text{O}$ values of samples in the M6 through C5 sequences is almost identical to that of $\delta^{18}\text{O}$ values of samples in the M3 through M5 sequences, except for one sample in the M6 sequence with a strikingly low value (Fig. 12).

Sr concentrations determined by ICP analysis of dissolved powders range from 0.014 to 0.090 wt % (Fig. 12). The mean value below the C4 sequence boundary is 0.0545 wt %, whereas the mean value above that boundary is

0.0494 wt %. The means do not differ significantly (Student's $t = 1.450$, $n_1 = 75$, $n_2 = 25$, $p = 0.15$).

Recognition of Subaerial Exposure in M6 through C5 Sequences

Just one instance in the data from Sequences M6 to C5 meets Criterion 1 for recognition of surfaces of subaerial exposure (see Methods). It is at the C4 sequence boundary, the horizon across which a statistically significant difference occurs in the entire set of $\delta^{13}\text{C}$ data (as discussed above). Seven instances fail to meet Criterion 1 but satisfy Criterion 2 (Fig. 12). Three of these are near, but none are at, the C1 sequence



Bluff Creek

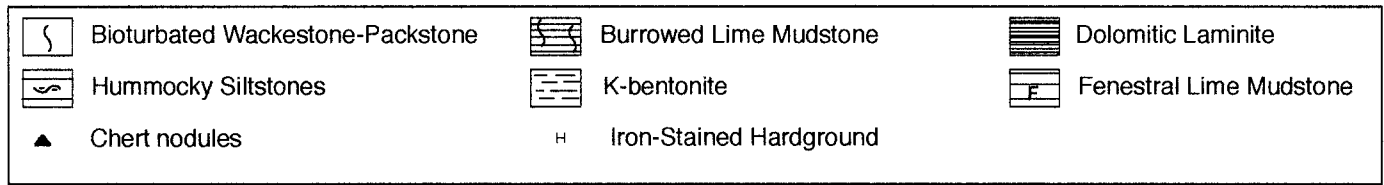


FIG. 11.—Stable C and O isotope composition and Sr concentration of micritic limestone in the M4 and M5 sequences at the Bluff Creek locality near Carthage, Tennessee. See caption of Figure 7 for explanation.

boundary. The others are at the C3 and C5 sequence boundaries and at parasequence tops in the C2 and C3 sequences. One instance fails to satisfy Criteria 1 and 2 but satisfies Criterion 3. It is below the C1 sequence boundary, just below the three horizons that meet Criterion 2 near that boundary (Fig. 12).

DISCUSSION

Surfaces of Subaerial Exposure or Marine Hardgrounds?

Two lines of argument lead us to interpret these surfaces as forming through subaerial exposure rather than as marine hardgrounds. First, although marine hardgrounds may be coated by cyanobacterial mats much like primitive soils (Krajewski 1984; Rasmussen et al. 1996), hardgrounds and soils would be expected to behave differently hydrologically, resulting in different geochemical expression. For a soil, meteoric water would have drained through the soil into the underlying carbonate, carrying with it the isotopically light carbon signature. Such downward advection of water would not be expected at a marine hardground, and as a result, a light carbon isotope spike might be developed immediately beneath a hardground, but not as a zone displaced below the surface (see Fig. 6). Furthermore, the lack of downward fluid flow and advection of isotopically light carbon at a marine hardground would not be expected to lead to a thick zone of isotopically light carbon beneath the surface, such as seen at many surfaces in this study.

Second, hardgrounds are far more numerous in the study interval, particularly within the M3–M4 interval, than are exposure surfaces identified by Criteria 1 to 3. If cyanobacterial coatings on marine hardgrounds were responsible for producing the $\delta^{13}\text{C}$ and Sr excursions seen in this study, interpreted exposure surfaces should be far more numerous. The scarcity of the interpreted exposure surfaces and their close association with surfaces suspected to be of subaerial origin based on sequence stratigraphic criteria argue for a subaerial origin.

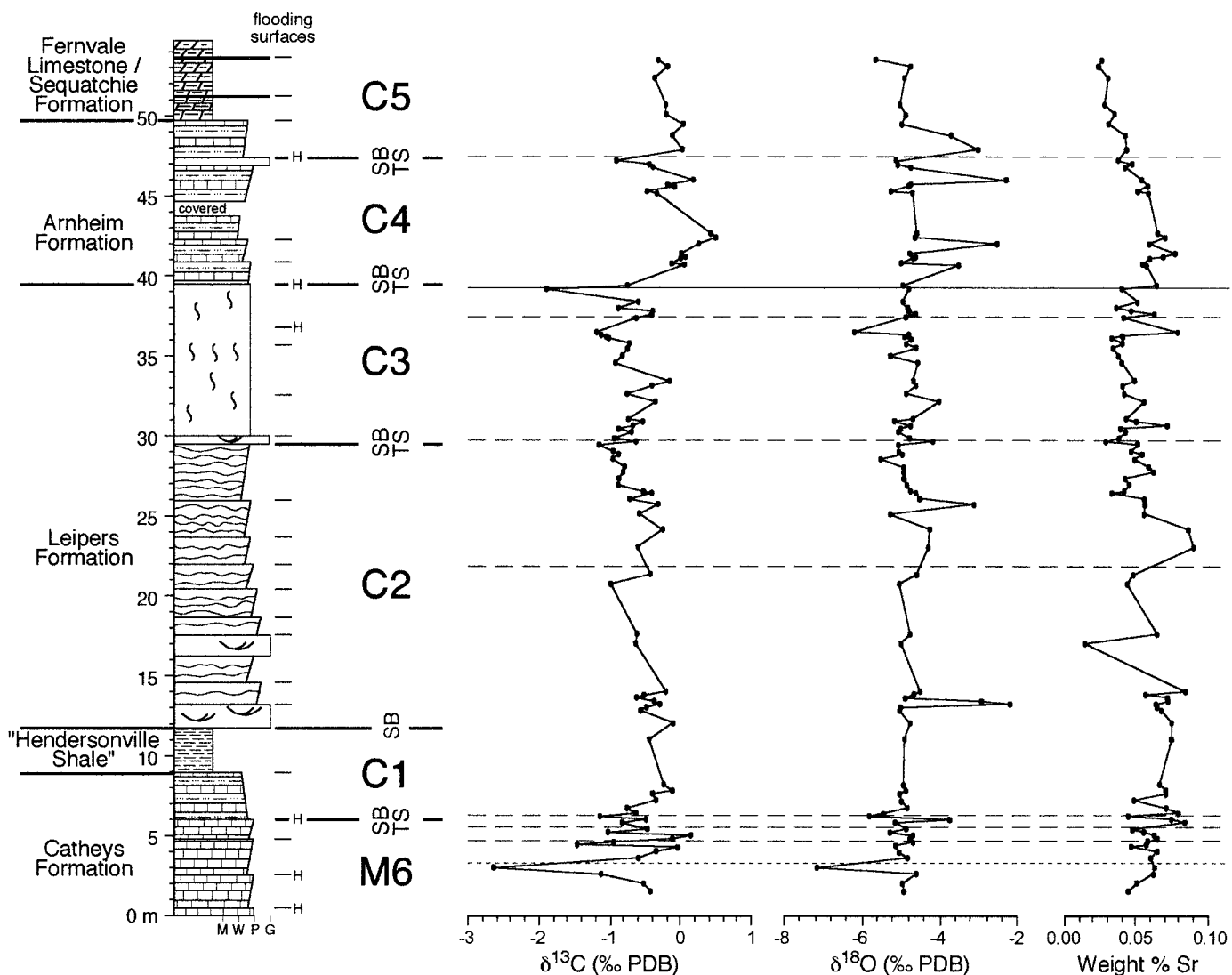
Surfaces of Subaerial Exposure and Sequence Stratigraphy

$\delta^{13}\text{C}$ and Sr data satisfying Criterion 1 confirm surfaces of subaerial exposure at the M5 and C4 sequence boundaries that were identified on

stratigraphic criteria by Holland and Patzkowsky (1997, 1998) (Figs. 7–12). Possible meteoric cements reported below those sequence boundaries (Díaz 1996; Jordan 1999; Hunter 2000) further support the contention that those horizons were surfaces of subaerial exposure and thus type I sequence boundaries. Those boundaries are the most pronounced sequence boundaries examined in this study, in that regional truncation can be documented at the M5 sequence boundary (Fig. 4), the M5 boundary has a microkarstic surface (fig. 5B of Holland and Patzkowsky 1998), and the C4 boundary is overlain by cobbles derived from the uppermost C3 sequence (fig. 5F of Holland and Patzkowsky 1998).

$\delta^{13}\text{C}$ and Sr data satisfying only Criteria 2 and 3 suggest surfaces of subaerial exposure at the C3 and C5 sequence boundaries, at correlative parasequence tops in the M4 sequence, and at parasequence tops in the C2 and C3 sequences. These surfaces lack microkarst or eroded cobbles, and regional truncation has been documented only at the C5 boundary (Fig. 5). At the parasequence tops in the M4 sequence, facies underlying the parasequence boundary indicate shallowing to supratidal environments, so subaerial exposure is not surprising. On the other hand, the surfaces of subaerial exposure suggested at parasequence tops in the C2 and C3 sequences are underlain by facies that provide no suggestion of shallowing to subaerial environments. This suggests short-term relative falls in sea level at a rate faster than tidal-flat progradation (Read et al. 1986). Subaerial exposure at tops of parasequences suggests that meter-scale cycles commonly interpreted as parasequences may actually represent higher-order sequences (e.g., Mitchum and Van Wagoner 1991; Holland et al. 1997).

The cluster of surfaces meeting Criteria 2 and 3 around the C1 sequence boundary may be the result of diagenetic overprinting that has obscured geochemical recognition of one truly significant sequence boundary. An alternate interpretation is that the strata around the interpreted M4 sequence boundary may represent a sequence boundary zone (Montañez and Osleger 1993) (Fig. 14). In this way, the boundary interval could be interpreted as containing a type II sequence boundary that failed to cause prolonged exposure of the carbonate platform, despite exposure at many of the higher order or meter-scale cycle boundaries. If this is true, some of the previously interpreted highstand systems tract might actually represent the shelf-margin systems tract (Fig. 1).



Vietnam Vets Highway

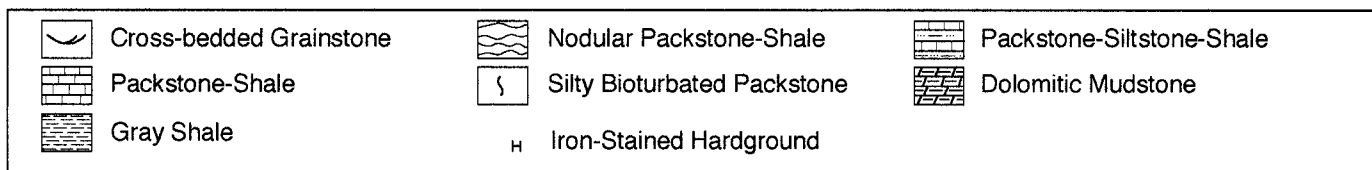


FIG. 12.—Stable C and O isotope composition and Sr concentration of micritic limestone in the M6 to C5 sequences at the Vietnam Veterans Highway locality on the north side of Nashville, Tennessee. See caption of Figure 7 for explanation.

Finally, a few apparent surfaces of subaerial exposure (e.g., in the M3 sequence at Hollis Creek) do not fall on previously recognized parasequence boundaries. These stratigraphically unpredicted surfaces of subaerial exposure suggest that subaerial exposure occurred more frequently than one would expect from the conventional placement of sequence and parasequence boundaries. These represent another type of “missed beat” in which high-frequency relative changes in sea level occurred but are not expressed by changes in facies, much as occurs in deeper subtidal missed beats (e.g., Goldhammer et al. 1993; Koerschner and Read 1989).

Variation along and Missing Section at the M5 Sequence Boundary

Pinchouts of the T3 (Deicke) and T4 (Millbrig) K-bentonites, as well as the pinchout of a parasequence beneath the M5 sequence boundary, indicate that more of the M4 sequence was removed by erosion at Columbia North and Nashville Airport than at Hollis Creek, Gladeville, and Bluff Creek (Fig. 15). The Columbia North and Nashville Airport sections also differ from the other three sections in that maximal $\delta^{13}\text{C}$ values below the M5 sequence boundary do not increase, and they differ from

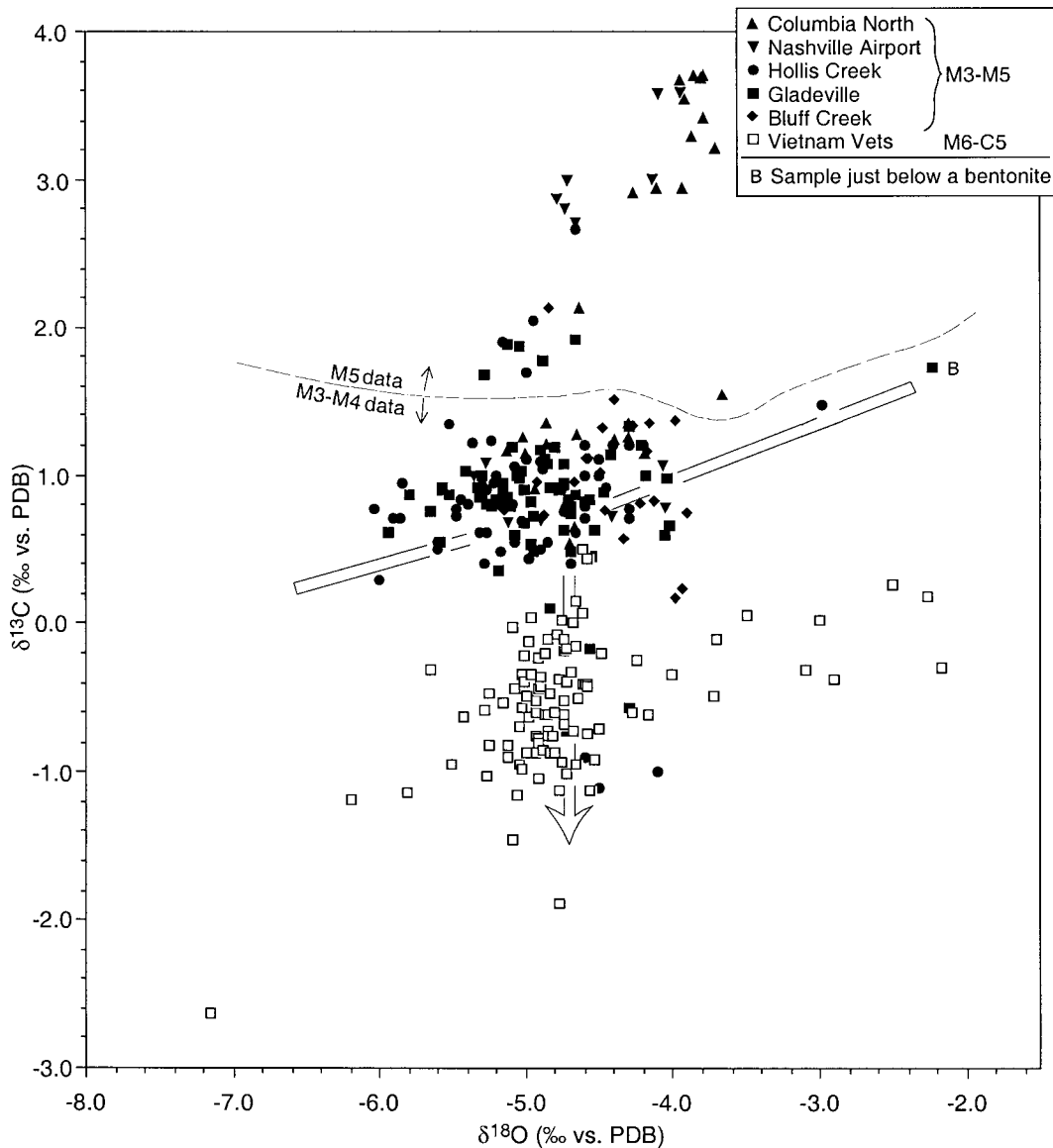


FIG. 13.—Plot of $\delta^{13}\text{C}$ and $\delta^{18}\text{O}$ values of limestone (largely micrite) samples from the M3 through M5 sequences (filled symbols) and M6 to C5 (open symbols). Open arrow and line summarize M3–M4 data's closest approximation of an "inverted J" distribution (Lohmann 1982, 1988); note that the data are more closely approximated by a T-shaped distribution.

the other three sections in having much greater $\delta^{13}\text{C}$ values above the M5 sequence boundary. These observations support reconstruction of a temporal trend of original (pedogenically unmodified) $\delta^{13}\text{C}$ (right side of Fig. 15). The resulting temporal trend shows a positive shift like that in the global compilation of $\delta^{13}\text{C}$ values by Veizer et al. (1999) and mimics the trend documented by Patzkowsky et al. (1997) in a stratigraphically more complete section in Pennsylvania. The results of this chemostratigraphic reconstruction suggest that the greater extent of missing section in the M4 sequence below the M5 sequence boundary is mirrored by a greater extent of missing section in the M5 sequence above that boundary. Such correspondence between the amount of time missing from sections above and below sequence boundaries confirms the relationships commonly depicted in Wheeler (chronostratigraphic) diagrams (Wheeler 1964) (e.g., Fig. 2).

Minima in $\delta^{13}\text{C}$ and Sr concentration are most recognizable at Bluff Creek, Gladeville, and Hollis Creek. Comparison with the flanks of the Nashville Dome (Fig. 15, inset) and lesser erosion (Fig. 15) suggest that

these localities were the most coastal or lowland sites of exposure in the Ordovician. Minima in $\delta^{13}\text{C}$ and Sr concentration are instead debatable or unrecognizable at Nashville Airport and Columbia North, which were subject to deeper erosion and, at least in the case of Columbia North, were the most paleo-inland sites (see inset of Fig. 15). It appears that faster rates of denudation at paleo-inland locations removed carbonate faster than it was altered, or that transgressive ravinement was more extensive there. On the other hand, lower rates of denudation and/or greater development of biological communities on the land surface allowed preservation of low- $\delta^{13}\text{C}$ and Sr-depleted limestone at the paleo-lowland sites. Thus, if the results below the M5 sequence boundary at Hollis Creek, Gladeville, and Bluff Creek show that $\delta^{13}\text{C}$ minima can be used to recognize subaerial exposure in Ordovician limestones, the results from Nashville Airport and Columbia North are a warning that such minima can sometimes fail to reveal subaerial exposure, especially in inland settings. Lack of $\delta^{13}\text{C}$ minima indicating exposure is therefore not necessarily evidence of lack of exposure itself.

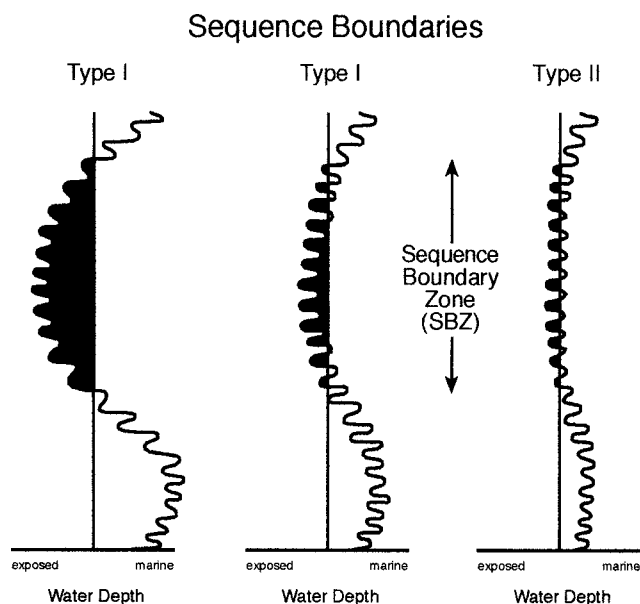


FIG. 14.—Potential expressions of sequence boundaries and associated subaerial exposure surfaces. In simplest case (left), a type I sequence boundary is developed and the carbonate platform is exposed during a single period of exposure. Higher-order cyclicality may cause additional minor exposure at several parasequences prior to and following the low-order type I sequence boundary (center). In cases in which the long-term rate of accommodation drops but does not become negative (right), the platform does not experience long-term exposure, but may be exposed only at higher-order cycle boundaries, resulting in a type II sequence boundary. Note that multiple exposure surfaces in the center and right cases may lead one to recognize a sequence boundary zone rather than a single sequence boundary. Furthermore, if the type I sequence boundary in the middle case does not experience more extensive meteoric diagenesis than the higher-order cycle boundaries, the middle and right cases may be indistinguishable in terms of both geochemical and stratigraphic expression.

Missing Intervals in the M6 through C5 Sequences

Data satisfying Criteria 1 to 3 suggest several possible surfaces of subaerial exposure in the M6 through C5 sequences (Fig. 12). Only at the C4 sequence boundary, however, does an abrupt change in average or maximum $\delta^{13}\text{C}$ suggest that a recognizable interval of time is not represented. The 0.6‰ increase in $\delta^{13}\text{C}$ at the C4 sequence boundary is compatible with a stratigraphic gap in the strongly increasing trend in the global compilation of $\delta^{13}\text{C}$ values by Veizer et al. (1999). Considerable erosion and nondeposition at the C4 boundary is also suggested by phosphate-coated cobbles of limestone derived from the uppermost C3 sequence (fig. 5F of Holland and Patzkowsky 1998) and by incised valleys at the C4 sequence boundary at the southern end of the Nashville Dome (Wilson 1948).

In contrast, the $\delta^{13}\text{C}$ record shows no significant offset at the C5 sequence boundary, even though that is the only boundary in the M6–C5 interval at which Holland and Patzkowsky (1998) inferred regional truncation of underlying stratigraphic units. The lack of offset may indicate that the C5 transition took place after the Caradoc to early Ashgill increase in the global oceanic $\delta^{13}\text{C}$ and during the Ashgill to Early Silurian stasis in $\delta^{13}\text{C}$ suggested by the compilation of Veizer et al. (1999).

Variation in Meteoric Signatures through Time

The maximum expression of meteoric diagenesis observed in this study's $\delta^{13}\text{C}$ data is a depletion of 2.4‰ below the M5 sequence boundary at Hollis Creek, and the maximum vertical extent of a $\delta^{13}\text{C}$ signature is 1.5 m at Bluff Creek. Both the amplitude and depth of these signatures are less than, and commonly less than half of, meteoric signatures observed in younger

carbonates (Table 1). That is hardly surprising, because identifiable macrofossils of land plants are not known from strata older than the Silurian, although cryptospores of bryophyte grade are known from rocks as old as the Llanvirn (Wellman and Gray 2000). However, microfossils of terrestrial microbial life are known from the Proterozoic (Horodyski and Knauth 1994), and Keller and Wood (1993) argued that limited microbial respiration can cause significant CO_2 concentrations in otherwise lifeless soils. The results of this study suggest that there was at least some biological community introducing ^{13}C -depleted CO_2 into the limestone regolith in the Mohawkian and Cincinnati, but that the extent of any such community was much less than that of later terrestrial plant communities. These results also make claims of low- $\delta^{13}\text{C}$ meteoric signatures as much as 50 m thick in Proterozoic carbonates (Beunias and Knauth 1985) all the more remarkable and bolster the questions raised by Vahrenkamp and Rossinsky (1987) about such signatures.

Accommodation Rates and Diagenetic Overprinting of Exposure Surfaces

Almost all samples in the M3 through M5 sequences have greater $\delta^{13}\text{C}$ values than samples from the M6 through C5 sequences; the only exceptions are samples just below the M5 sequence boundary that we would interpret to have been pedogenically modified (see above). Comparison with the global compilation of $\delta^{13}\text{C}$ values by Veizer et al. (1999) would predict the opposite, in that $\delta^{13}\text{C}$ of brachiopods, and by extension presumably $\delta^{13}\text{C}$ of seawater HCO_3^- , increased by about 2‰ from M3–M5 to M6–C5 time.

There are at least two possible explanations of this paradox. One explanation, of which we are skeptical, assumes that the bulk of the Nashville $\delta^{13}\text{C}$ values are largely unaltered or at most equally altered from their original compositions, and that conditions on the Nashville Dome changed from seawater locally enriched in ^{13}C relative to the global mean in M3–M5 time to seawater locally depleted in ^{13}C relative to the global mean in M6–C5 time. That explanation is seemingly supported by the interpretation by Holland and Patzkowsky (1997, 1998) that the change from tropical-type Mohawkian carbonates to temperate-type Cincinnati carbonates was the result of increased upwelling of deep waters. In the modern oceans, the $\delta^{13}\text{C}$ of dissolved CO_2 in deep waters is commonly 1.0‰ less than that of surface waters and can be 2.2‰ less (Kroopnick 1985). However, if the global average $\delta^{13}\text{C}$ of seawater CO_2 increased by 1.8‰ from M4 time to M6–C5 time while upwelling caused a local 2.0‰ decrease independent of the global increase, that combination could explain part of, but not all of, the observed 1.4‰ decrease observed in our samples. A 1.4‰ decrease in local seawater $\delta^{13}\text{C}$ due to upwelling during a global 1.8‰ increase would require a $\delta^{13}\text{C}$ difference between deep water and surface water of 3.2‰, which is well beyond any such difference observed in the modern ocean. The Ordovician ocean could have had a greater difference between shallow and deep water, but $\delta^{13}\text{C}$ values of brachiopods from a coeval shallow-to-deep transect in New York have at most a 1.5‰ difference (Railsback 1989).

A second and more likely explanation of the lower $\delta^{13}\text{C}$ values in the M6 through C5 sequences than those in the M3 through M5 sequences is that the relatively thin M6 to C5 sequences underwent more thorough and repeated penetration of pedogenic low- $\delta^{13}\text{C}$ meteoric waters to shift the isotopic composition of essentially all the limestone in that interval. This explanation would account for the general uniformity of $\delta^{13}\text{C}$ values above the C4 sequence boundary and below it and for the apparent lack of offset in $\delta^{13}\text{C}$ values above and below the C5 boundary (as discussed above). It would also explain the uniformly low Sr concentrations in the M6 through C5 sequences (as compared to the range of Sr concentrations in the M3 through M5 sequences) as the result of more thorough early leaching of originally aragonitic phases.

If we are correct that diagenetic overprinting (Whitaker et al. 1997) was

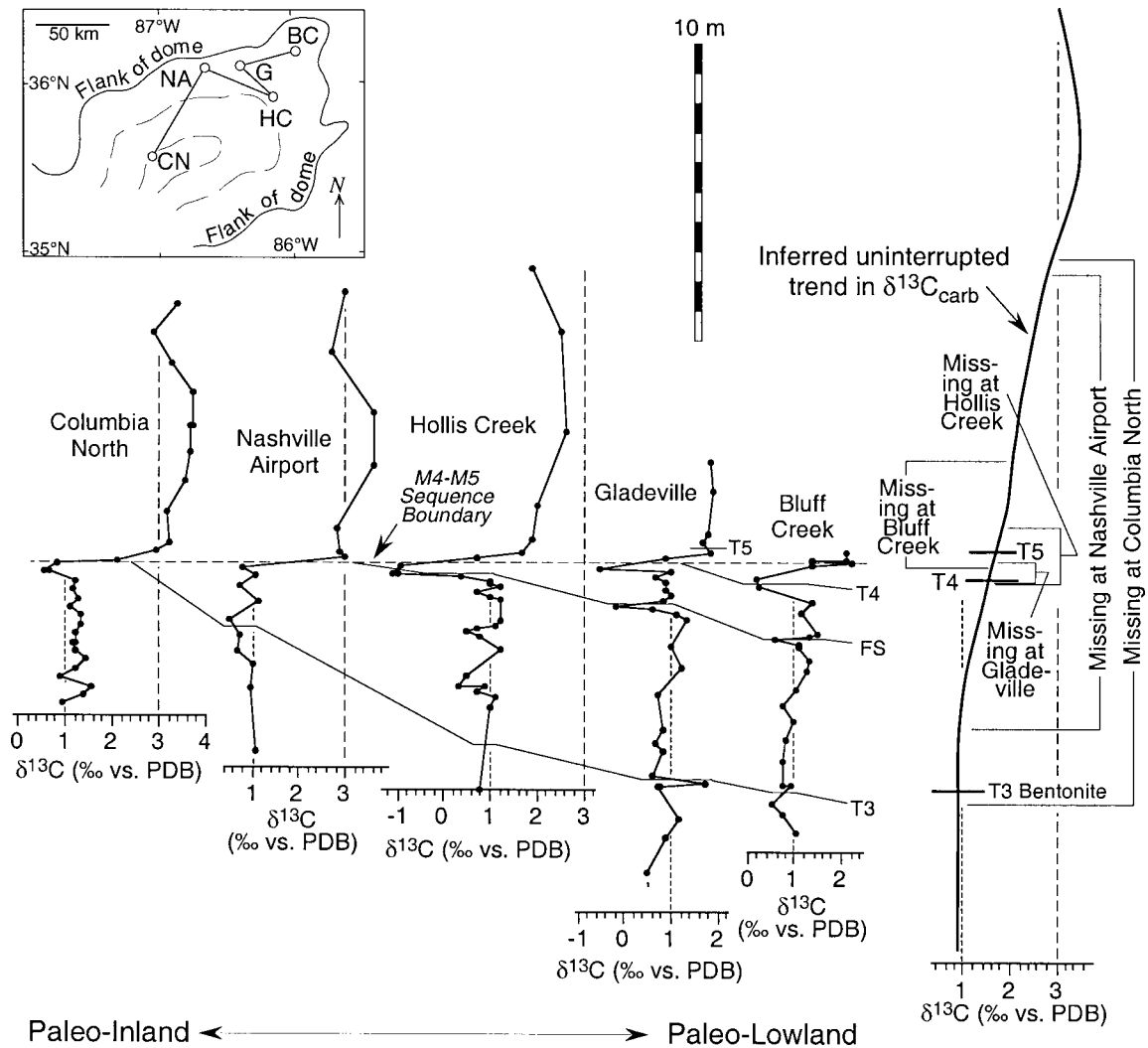


FIG. 15.— $\delta^{13}\text{C}$ of limestones, largely micrites, above and below the M5 sequence boundary (cf. Fig. 4). The inferred uninterrupted $\delta^{13}\text{C}$ trend at right was constructed solely by sequential overlay of the inferred trend on the data at left, with addition of segments to account for ranges of $\delta^{13}\text{C}$ not present in the data. It is the shortest parsimonious reconstruction possible. Incorporating abrupt increases in the curve could make shorter reconstructions; incorporating decreases or intervals of no change could make longer reconstructions. Inset map shows location of outcrops and the "Ordovician–Silurian" flank of the Nashville Dome inferred by Stearns and Reesman (1986) from structural analysis.

significant in the M6 through C5 sequences, then it appears that differing rates of accommodation were an important control on early diagenesis of these strata. In the M3 through M5 sequences, relatively fast accommodation with continued sediment accumulation may have allowed most strata to sink below the level of significant penetration by later episodes of meteoric influx. In the C1 through C5 sequences, on the other hand, much slower accommodation rates and accompanying low rates of sediment accumulation may have kept strata at sufficiently shallow depths to allow repeated infiltration during subsequent episodes of subaerial exposure, including the long terminal Ordovician lowstand with its estimated duration of 3 My (based on the time scale of Fordham 1992). Although accommodation rates remained high during deposition of the M6 sequence, slow accommodation and sediment accumulation during deposition of the C1 sequence would have held the M6 deposits in the realm of meteoric diagenesis long enough to give them the same general diagenetic characteristics as those of C1 to C5 strata.

Despite possible overprinting, evidence of subaerial exposure meeting at least Criterion 3 was preserved at four of the five sequence boundaries in the M6–C5 interval. Overprinting was thus not complete. The model of

Whitaker et al. (1997) used eustatic changes based on the icehouse conditions of the Quaternary, with roughly 100 m fluctuations in sea level every 110,000 years, and led to the conclusion that overprinting should eliminate geochemical signatures of subaerial exposure. The persistence of such signatures in the M6–C5 interval suggests that modeling with different inputs could profitably be employed to explore the potential for overprinting during greenhouse periods such as the late (but not latest) Ordovician, in which the magnitude of sea-level fluctuations may be much less and in which the duration of sea-level fluctuations may differ from that in icehouse periods.

Trends in Diagenetic Data

One of the hallmarks of C and O isotope data from carbonates influenced by meteoric diagenesis is an "inverted J"-shaped trend in such data (Lohmann 1982, 1988). This trend has been interpreted in studies like this one of stratigraphically distributed macroscopic samples (e.g., Fouke et al. 1996), although the trend was originally found in microscopic sampling of cement zones (Lohmann 1982, 1988; figure 3 of Melim et al. 1995). In

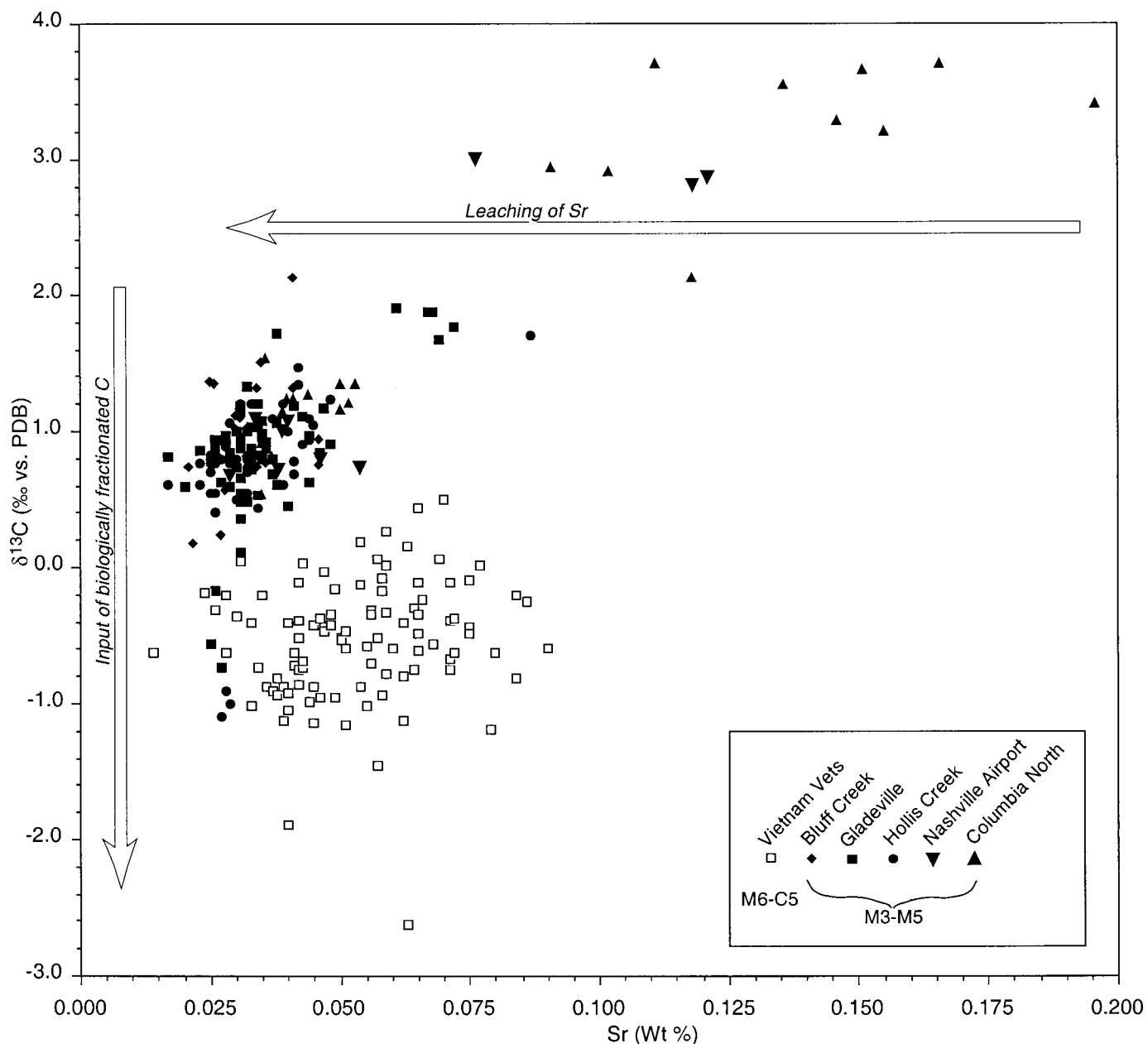


FIG. 16.—Plot of Sr concentrations and $\delta^{13}\text{C}$ values of limestone (largely micrite) samples from the M3 through M5 sequences (filled symbols) and M6 to C5 (open symbols). Open arrows indicate processes interpreted to account for observed trends that form an inverted J. Data from the M6 through C5 sequences do not follow any such curve and are interpreted to all lie at the lower left end of such a curve.

this study, data from the M3 and M4 sequences may follow a modified J-shaped curve on a $\delta^{18}\text{O}$ – $\delta^{13}\text{C}$ plot, but they are better described by a T-shaped distribution resulting from a broad range in $\delta^{18}\text{O}$ values (Fig. 13). $\delta^{18}\text{O}$ and $\delta^{13}\text{C}$ data from the M6 through C5 sequences do not follow any trend comparable to an inverted J.

One plot on which the inverted-J curve does emerge in this study is a plot of $\delta^{13}\text{C}$ and Sr concentration (Fig. 16). This trend is to be expected if one assumes a starting composition with relatively high Sr concentrations because of inclusion of at least some aragonitic components and with $\delta^{13}\text{C}$ values near zero on account of a marine origin. Dissolution of aragonite removes Sr so readily that most samples deviate from the original value, but $\delta^{13}\text{C}$ is changed less because of low water–rock ratios (Banner and Hanson 1990), leading to the inverted J seen in data from the M3 through

M5 sequences (Fig. 16). Repeated influx of meteoric water into the M6 through C5 sequences seems instead to have left all samples from those sequences plotting at the lower left end of the inverted J.

CONCLUSIONS

1) Carbon isotope and Sr concentration data screened by our most stringent criterion, Criterion 1, support the inference of subaerial exposure at the M5 and C4 third-order sequence boundaries identified by Holland and Patzkowsky (1997, 1998). Data satisfying less stringent criteria support the inference of subaerial exposure at or near the M4, C1, C3, and C5 sequence boundaries. Most sequence boundaries are characterized by a single surface of exposure, but the C1 boundary has a cluster of exposure surfaces and may represent a sequence boundary zone.

TABLE 1.—Stratigraphic carbon isotope signatures of subaerial exposure.

Age	Location	Amplitude (%)	Depth (m)	Reference
Pleistocene	San Salvador	4 to 9	~2	Beier (1987)
Pleistocene	Barbados	4 to 6	~4	Allan and Matthews (1982)
Cretaceous	France	2.3	14	Fouke et al. (1996)
Cretaceous	Texas	4.5	1	Allan and Matthews (1982)
Cretaceous	Texas	~4	3 to 4	Allan and Matthews (1982)
Pennsylvanian	New Mexico	3 to 8	5 to 15	Algeo (1996)
Pennsylvanian	New Mexico	1 to 2.5	≤3	Goldstein (1991)
Pennsylvanian	Texas	~4	5	Allan and Matthews (1982)
Mississippian	Kentucky	2 to 3	2.5	Allan and Matthews (1982)
Ordovician	Tennessee	0 to 2.4	0 to 1.5	This paper
Proterozoic	Arizona	3	50	Beunas and Knauth (1985)
Archean	South Africa	5*	5.5	Watanabe et al. (2000)

* Developed on parent rock interpreted to be carbonate-free.

2) Application of Criterion 2 suggests surfaces of subaerial exposure at the top of three parasequences, indicating that these parasequences may be better interpreted as high-frequency sequences. Other surfaces suggested by Criteria 2 and 3 occur at neither recognized sequence boundaries nor at parasequence boundaries; these may represent a type of missed beat, in which sea-level fluctuations are preserved geochemically but not recognized by changes in facies or stacking patterns. Our results thus confirm the previously identified third-order sequence boundaries but additionally reveal higher-order sequence boundaries and so provide greater sequence-stratigraphic resolution.

3) The vertical extent of samples with low $\delta^{13}\text{C}$ at our inferred surfaces of subaerial exposure suggests that they are not simply marine hardgrounds at which cyanobacterial mats formed.

4) This study used a smaller sampling interval than that in many analogous studies of subaerial exposure. This study's recognition of many stratigraphically unpredicted surfaces of subaerial exposure suggests that small sampling intervals may be more appropriate in such studies.

5) Different sequence boundaries exhibit different degrees of geochemical alteration, and more extensive alteration appears to characterize sequence boundaries of greater temporal significance.

6) Overprinting of exposure surfaces is strongly correlated with low accommodation rates as estimated previously from the backstripping of measured sections. In the M6 through C5 sequences, which were deposited during slow accommodation, only one sequence boundary satisfies Criterion 1, possibly because wholesale alteration of the section by repeated episodes of meteoric diagenesis precludes recognition of distinct surfaces.

7) Geochemical expression of subaerial exposure is strongly controlled by position on platform. In this study, minima in $\delta^{13}\text{C}$ and Sr concentration were best preserved in paleo-coastal areas. Such minima are poorly developed in paleo-inland areas, cautioning against using the lack of such minima to argue against subaerial exposure.

8) The extent of depletion of ^{13}C below this study's inferred surfaces of subaerial exposure is less than that of meteoric signatures in younger carbonates (Table 1), presumably because of the lesser development of biological communities in Ordovician soils.

9) It may not be reasonable to expect an "inverted J" curve in $\delta^{18}\text{O}$ – $\delta^{13}\text{C}$ plots of stratigraphically dispersed bulk or macroscopic samples. An inverted J in Sr– $\delta^{13}\text{C}$ plots may be a more reasonable criterion for recognition of meteoric diagenesis in such samples.

ACKNOWLEDGMENTS

We thank members of Railsback's 1996 and 2000 Carbonate Petrology classes for their efforts on class projects incorporated in this paper. We also thank Christopher J. Fleisher and William R. McClain of the University of Georgia Department of Geology for their help with microprobe and isotopic analyses, respectively. Jordan and Hunter acknowledge the generous support of the University of Georgia Department of Geology Watts-Wheeler Scholarship Fund. Reviews by Drs. Thomas J. Algeo, Leslie Melim, Ezat Heydari, and David A. Budd and editing by Dr. John B.

Southard all greatly improved the manuscript. The data described in this paper and referenced as Appendix 1 have been archived and are available in digital form at the World Data Center for Marine Geology and Geophysics, Boulder, NOAA/NGDC E/GC3, 325 Broadway, Boulder, CO 80305 USA; URL: <http://www.ngdc.noaa.gov/mgg/sepm/archive/index.html>, e-mail: wcdmagg@noaa.gov.

REFERENCES

- ALGEO, T.J., 1996, Meteoric water/rock ratios and the significance of sequence and parasequence boundaries in the Gobbler Formation (Middle Pennsylvanian) of south-central New Mexico, in Witzke, B.J., Ludvigson, G.A., and Day, J., eds., *Paleozoic Sequence Stratigraphy: Views from the North American Craton*: Geological Society of America, Special Paper 306, p. 359–371.
- ALLAN, R.A., AND MATTHEWS, R.K., 1982, Isotope signatures associated with early meteoric diagenesis: *Sedimentology*, v. 29, p. 797–817.
- BANNER, J.L., AND HANSON, G.N., 1990, Calculation of simultaneous isotopic and trace element variations during water–rock interactions with application to carbonate diagenesis: *Geochimica et Cosmochimica Acta*, v. 54, p. 3123–3137.
- BEEUNAS, M.A., AND KNAUTH, L.P., 1985, Preserved stable isotopic signature of subaerial diagenesis in the 1.2-b.y. Mescal Limestone, central Arizona: implications for the timing and development of a terrestrial plant cover: *Geological Society of America, Bulletin*, v. 96, p. 737–745.
- BERNER, R.A., 1994, GEOCARB II: A revised model of atmospheric CO_2 over Phanerozoic time: *American Journal of Science*, v. 294, p. 56–91.
- BROWN, R.G., 1997, Petrogenesis and rock packaging of Middle Ordovician carbonates, Black River Group, southeastern Ontario, Canada [M.S. Thesis]: Queen's University, Kingston, Ontario, 158 p.
- DIÁZ, J.R., 1996, Meteoric diagenesis of Ordovician limestones from Cannon County, Tennessee [M.S. Thesis]: University of Georgia, 70 p.
- FORDHAM, B.G., 1992, Chronometric calibration of mid-Ordovician to Tournaisian conodont zones: a compilation from recent graphic-correlation and isotope studies: *Geological Magazine*, v. 129, p. 709–721.
- FOUKE, B.W., EVERTS, A.-J.W., ZWART, E.W., SCHLAGER, W., SMALLEY, P.C., AND WEISSERT, H., 1996, Subaerial exposure unconformities on the Vercors carbonate platform (SE France) and their sequence stratigraphic significance, in Howell, J.A., and Aiken, J.F., eds., *High Resolution Sequence Stratigraphy: Innovation and Application*: Geological Society of London, Special Publication 104, p. 295–320.
- GOLDHAMMER, R.K., LEHMANN, P.J., AND DUNN, P.A., 1993, The origin of high-frequency platform carbonate cycles and third-order sequences (Lower Ordovician El Paso Group, west Texas): constraints from outcrop data and stratigraphic modeling: *Journal of Sedimentary Petrology*, v. 63, p. 318–359.
- GOLDSTEIN, R.H., 1991, Stable isotope signatures associated with paleosols, Pennsylvanian Holder Formation, New Mexico: *Sedimentology*, v. 38, p. 67–77.
- GROVER, G.A., JR., AND READ, J.F., 1983, Paleoquifer and deep burial related cements defined by regional cathodoluminescent patterns, Middle Ordovician carbonates, Virginia: *American Association of Petroleum Geologists, Bulletin*, v. 67, p. 1275–1303.
- HOLLAND, S.M., AND PATZKOWSKY, M.E., 1997, Distal orogenic effects on peripheral bulge sedimentation; Middle and Upper Ordovician of the Nashville Dome: *Journal of Sedimentary Research*, v. 67, p. 250–263.
- HOLLAND, S.M., AND PATZKOWSKY, M.E., 1998, Sequence stratigraphy and relative sea-level history of the Middle and Upper Ordovician of the Nashville Dome, Tennessee: *Journal of Sedimentary Research*, v. 68, p. 684–699.
- HOLLAND, S.M., MILLER, A.I., DATILO, B.F., MEYER, D.L., AND DIEKMEYER, S.L., 1997, Cycle anatomy and variability in the storm-dominated type Cincinnati (Upper Ordovician): coming to grips with cycle delineation and genesis: *Journal of Geology*, v. 105, p. 135–152.
- HORODYSKI, R.J., AND KNAUTH, L.P., 1994, Life on land in the Precambrian: *Science*, v. 263, p. 494–498.
- HUNTER, D.M., 2000, Testing for subaerial exposure at five Upper Ordovician sequence boundaries, Nashville Dome, Tennessee [M.S. Thesis]: University of Georgia, 228 p.
- JORDAN, E.M., 1999, Using isotopic and petrographic analyses to recognize subaerial exposure in Ordovician limestones from central Tennessee [M.S. Thesis]: University of Georgia, 160 p.
- KELLER, C.K., AND WOOD, B.D., 1993, Possibility of chemical weathering before the advent of vascular land plants: *Nature*, v. 364, p. 223–225.
- KHER, S., 1996, Patterns of meteoric diagenesis in the Middle and Late Ordovician carbonates of the Southern Appalachians [Ph.D. Dissertation]: Florida State University, 181 p.
- KOERSCHNER, W.F., AND READ, J.F., 1989, Field and modeling studies of Cambrian carbonate cycles, Virginia Appalachians: *Journal of Sedimentary Petrology*, v. 59, p. 654–687.
- KRAJEWSKI, K.P., 1984, Early diagenetic phosphate cements in the Albian condensed glauconitic limestone of the Tatra Mountains, Western Carpathians: *Sedimentology*, v. 31, p. 443–470.
- KROOPNICK, P.M., 1985, The distribution of ^{13}C in the world oceans: *Deep-Sea Research*, v. 32, p. 57–84.
- LASEMI, Z., AND SANDBERG, P.A., 1994, Temporal trends in the mineralogy of Phanerozoic micrite precursors (abstract): AAPG/SEPM Annual Meeting, Abstracts, p. 193.
- LOHMANN, K.C., 1982, "Inverted J" carbon and oxygen isotopic trends; a criterion for shallow meteoric phreatic diagenesis (abstract): Geological Society of America, Abstracts with Programs, v. 14, p. 548.
- LOHMANN, K.C., 1988, Geochemical patterns of meteoric diagenetic systems and their application to studies of paleokarst, in James, N.P., and Choquette, P.W., eds., *Paleokarst*: New York, Springer-Verlag, p. 58–80.

- McCREA, J.M., 1950, The isotopic composition of carbonates and a paleotemperature scale: *Journal of Chemical Physics*, v. 18, p. 849–857.
- MELIM, L.A., SWART, P.K., AND MALIVA, R.G., 1995, Meteoric-like fabrics forming in marine waters: implications for the use of petrography to identify diagenetic environments: *Geology*, v. 23, p. 755–758.
- MITCHUM, R.M., AND VAN WAGONER, J.C., 1991, High-frequency sequences and their stacking patterns: Sequence-stratigraphic evidence of high-frequency eustatic cycles: *Sedimentary Geology*, v. 70, p. 131–160.
- MONTANEZ, I.P., AND OSLEGER, D.A., 1993, Parasequence stacking patterns, third-order accommodation events, and sequence stratigraphy of Middle to Upper Cambrian platform carbonates, Bonanza King Formation, Southern Great Basin, in Loucks, R.G., and Sarg, J.F., ed., *Carbonate Sequence Stratigraphy*: American Association of Petroleum Geologists, Memoir 57, p. 305–326.
- PATZKOWSKY, M.E., AND HOLLAND, S.M., 1999, Biofacies replacement in a sequence stratigraphic framework: Middle and Upper Ordovician of the Nashville Dome, Tennessee, USA: *Palaios*, v. 14, p. 301–323.
- PATZKOWSKY, M.E., SŁUPIK, L.M., ARTHUR, M.A., PANCOST, R.D., AND FREEMAN, K.H., 1997, Late Middle Ordovician environmental change and extinction: Harbinger of the Late Ordovician or continuation of Cambrian patterns?: *Geology*, v. 25, p. 911–914.
- POSAMENTIER, H.W., AND JAMES, D.P., 1993, An overview of sequence-stratigraphic concepts: uses and abuses: *International Association of Sedimentologists, Special Publication 18*, p. 3–18.
- RAILSBACK, L.B., 1989, Ordovician paleoceanography: stable isotope and C–S–Fe evidence from the Caradocian Trenton Group, Mohawk Valley, New York [Ph.D. Dissertation]: University of Illinois, 138 p.
- RASMUSSEN, K.A., ROMANOVSKY, V.V., MACINTYRE, I.G., AND PRUFERT, L., 1996, Late Quaternary coastal microbialites and beachrocks of Lake Issyk-Kul, Kyrgyzstan: geologic, hydrographic, and climatic significance (abstract): *Geological Society of America, Abstracts with Programs*, v. 28, p. 304.
- READ, J.F., GROTZINGER, J.P., BOVA, J.A., AND KOERSCHNER, W.F., 1986, Models for generation of carbonate cycles: *Geology*, v. 14, p. 107–110.
- SANDBERG, P.A., 1983, An oscillating trend in Phanerozoic non-skeletal mineralogy: *Nature*, v. 305, p. 19–22.
- STEARNS, R.G., AND REESMAN, A.L., 1986, Cambrian to Holocene structural and burial history of the Nashville Dome: *American Association of Petroleum Geologists, Bulletin*, v. 70, p. 143–154.
- SWART, P.K., BURNS, S.J., AND LEDER, J.J., 1991, Fractionation of the stable isotopes of oxygen and carbon in carbon dioxide during the reaction of calcite with phosphoric acid as a function of temperature and technique: *Chemical Geology*, v. 86, p. 89–96.
- TOBIN, K.J., AND WALKER, K.R., 1994, Meteoric diagenesis below a submerged platform: implications for $\delta^{13}\text{C}$ compositions prior to pre-vascular plant evolution, Middle Ordovician, Alabama, U.S.A.: *Sedimentary Geology*, v. 90, p. 95–111.
- VAHRENKAMP, V.C., AND ROSSINSKY, V., JR., 1987, Preserved stable isotopic signature of subaerial diagenesis in the Mescal Limestone, central Arizona: implications for the timing of a terrestrial plant cover—Discussion: *Geological Society of America, Bulletin*, v. 99, p. 595–597.
- VAN WAGONER, J.C., MITCHUM, R.M., CAMPION, K.M., AND RAHMANIAN, V.D., 1990, Siliciclastic sequence stratigraphy in well logs, cores, and outcrops: Concepts for high-resolution correlation of time and facies: *American Association of Petroleum Geologists, Methods in Exploration Series, No. 7*, 55 p.
- VEIZER, J., ALA, D., AZMY, K., BRUCKSCHEN, P., BUHL, D., BRUHN, F., CARDEN, G.A.F., DIENER, A., EBNETH, S., JASPER, T., KORTE, C., PAWELLEK, F., PODLAHA, O.G., AND STRAUSS, H., 1999, $^{87}\text{Sr}/^{86}\text{Sr}$, $\delta^{13}\text{C}$ and $\delta^{18}\text{O}$ evolution of Phanerozoic seawater: *Chemical Geology*, v. 161, p. 59–88.
- WATANABE, Y., MARTINI, J.E., AND OHMOTO, H., 2000, Geochemical evidence for terrestrial ecosystems 2.6 billion years ago: *Nature*, v. 408, p. 574–578.
- WELLMAN, C.H., AND GRAY, J., 2000, The microfossil record of early land plants: *Royal Society of London, Philosophical Transactions, Biological Sciences*, v. 355, p. 717–732.
- WHEELER, H.E., 1964, Baselevel, lithosphere surface, and time stratigraphy: *Geological Society of America, Bulletin*, v. 75, p. 599–610.
- WHITAKER, F., SMART, P., HAGUE, Y., WALTHAM, D., AND BOSENCE, D., 1997, Coupled two-dimensional diagenetic and sedimentological modeling of carbonate platform evolution: *Geology*, v. 25, p. 175–178.
- WILKINSON, B.H., AND GIVEN, R.K., 1986, Secular variation in abiotic marine carbonates: Constraints on Phanerozoic atmospheric carbon dioxide contents and oceanic Mg/Ca ratios: *Journal of Geology*, v. 94, p. 321–333.
- WILSON, C.W., JR., 1948, Channels and channel-filling sediments of Richmond age in south-central Tennessee: *Geological Society of America, Bulletin*, v. 59, p. 733–765.

Received 30 July 2001; accepted 5 February 2003.